

Article

Geometallurgy of Cobalt Black Ores in the Katanga Copperbelt (Ruashi Cu-Co Deposit): A New Proposal for Enhancing Cobalt Recovery

Pascal Mambwe ^{1,2,3,*}, Michel Shengo ⁴ , Théophile Kidyanyama ^{3,5}, Philippe Muchez ¹  and Mumba Chabu ³

¹ Department of Earth and Environmental Sciences, Katholieke Universiteit Leuven, Celestijnenlaan 200E, 3001 Leuven, Belgium; philippe.muchez@kuleuven.be

² Department of Exploration Geology, Tenke Fungurume Mining S.A., Kolwezi, Democratic Republic of the Congo

³ Department of Geology, Faculty of Sciences, University of Lubumbashi, Lubumbashi 1825, Democratic Republic of the Congo; theophil.ngoy@ruashi.com (T.K.); chabu.cm@gmail.com (M.C.)

⁴ Department of Chemistry, Faculty of Sciences, University of Lubumbashi, Lubumbashi 1825, Democratic Republic of the Congo; shengolutandulamichel@yahoo.fr

⁵ Department of Mine Geology, Ruashi Mining S.A, Lubumbashi, Democratic Republic of the Congo

* Correspondence: pascal.mambwematanda@kuleuven.be; Tel.: +243-810242310

Abstract: Copper-cobalt deposits in the Central African Copperbelt belong to the Sediment-Hosted Stratiform Copper (SHSC) type and are situated in the Neoproterozoic Katanga Supergroup. This paper describes in detail the geology, geochemistry and hydrometallurgy of cobalt, with a special focus on the Black Ore Mineralised Zone (BOMZ) unit from the Ruashi Cu-Co deposit as a case study. Based on results from fieldwork and laboratory testing, it was concluded that the BOMZ consists of a succession of massive and stratified dolostones, which are weathered into carbonaceous clay dolostones and clays. The Lower “Calcaire à Minéraux Noirs Formation” (Lower CMN Formation) consists of stratified and finely laminated dolostones, which are weathered at the surface into clayey to siliceous dolostones. The cobalt concentration in the weathering zone is due to supergene enrichment, a process that is linked to the formation of a cobalt cap. The ore consists of heterogenite associated with minor amounts of chrysocolla and malachite. Minor carrollite, chalcopyrite, chalcocite and bornite are present in unweathered fragments. The cobalt grade in both the BOMZ and Lower CMN decreases within depth while the copper grade increases. These grade changes reflect the variation in mineralogy with depth from heterogenite with minor amounts of malachite and chrysocolla to malachite, chrysocolla with traces of heterogenite, spherocobaltite, chalcocite, chalcopyrite, carrollite and bornite. Based on the Cu (100^x AS Cu/TCu) and Co ratio (100^x AS Co/TCo), which is related to the ore mineralogy, oxide ores (Cu ratio ≥ 75%) and oxide dominant mixed ores (Cu ratio < 75%, containing the copper sulphide chalcocite) can be differentiated in both the BOMZ and Lower CMN. The absence of talc and the low concentration of Ni, Mn and Fe, on the one hand, and the high-grade Cu in the BOMZ, on the other hand, facilitate the hydrometallurgy of cobalt but require a specific processing. Consequently, the recovery of Co from the BOMZ requires the application of a processing method that is based on sulphuric acid (30 g/L) leaching under reducing conditions (300–350 mV) and the removal of impurities (Cu > 95% and Mn ≈ 99%) from the pregnant leach solution (PLS) by solvent extraction (SX) prior to the precipitation of cobalt as a high-grade hydroxide (40.5%). The sulphuric acid leaching of the BOMZ enabled achieving, after 8 h of magnetic stirring (500 rpm), a highest yield of 93% Co, with other major elements Mn (84%) and Cu (40%). The latter forms a main co-product of the Co exploitation. In contrast, the highest leaching yield for Fe remained smaller than 5%.

Keywords: cobalt; copper; ore mineralogy; geochemistry; hydrometallurgy; Katanga Copperbelt



Citation: Mambwe, P.; Shengo, M.; Kidyanyama, T.; Muchez, P.; Chabu, M. Geometallurgy of Cobalt Black Ores in the Katanga Copperbelt (Ruashi Cu-Co Deposit): A New Proposal for Enhancing Cobalt Recovery. *Minerals* **2022**, *12*, 295. <https://doi.org/10.3390/min12030295>

Academic Editors: Quentin Dehaine and Alan R. Butcher

Received: 30 December 2021

Accepted: 24 February 2022

Published: 26 February 2022

Publisher's Note: MDPI stays neutral with regard to jurisdictional claims in published maps and institutional affiliations.



Copyright: © 2022 by the authors. Licensee MDPI, Basel, Switzerland. This article is an open access article distributed under the terms and conditions of the Creative Commons Attribution (CC BY) license (<https://creativecommons.org/licenses/by/4.0/>).

1. Introduction

The Central African Copperbelt (CACB) hosts the Sediment-Hosted Stratiform Copper Deposits (SHSC) in the Neoproterozoic Katanga Supergroup (Figure 1; [1–5]). The CACB contains around 75% of the world's Co reserve, with around 60% sourced from the DR Congo [6–10]. Around 25% of world Co reserves are hosted in other types of deposits, for example, Co occurs often associated with Ni, Cu, PGE, and REE in mafic and ultramafic rocks as well as ore mineralization. In addition, it is found in Ni-Fe residual lateritic and volcanogenic deposits [6,11–13]. Due to the increased demand of Co in the electric vehicle industry for batteries, and the high technology industries, Co has become a critical metal [14–17].

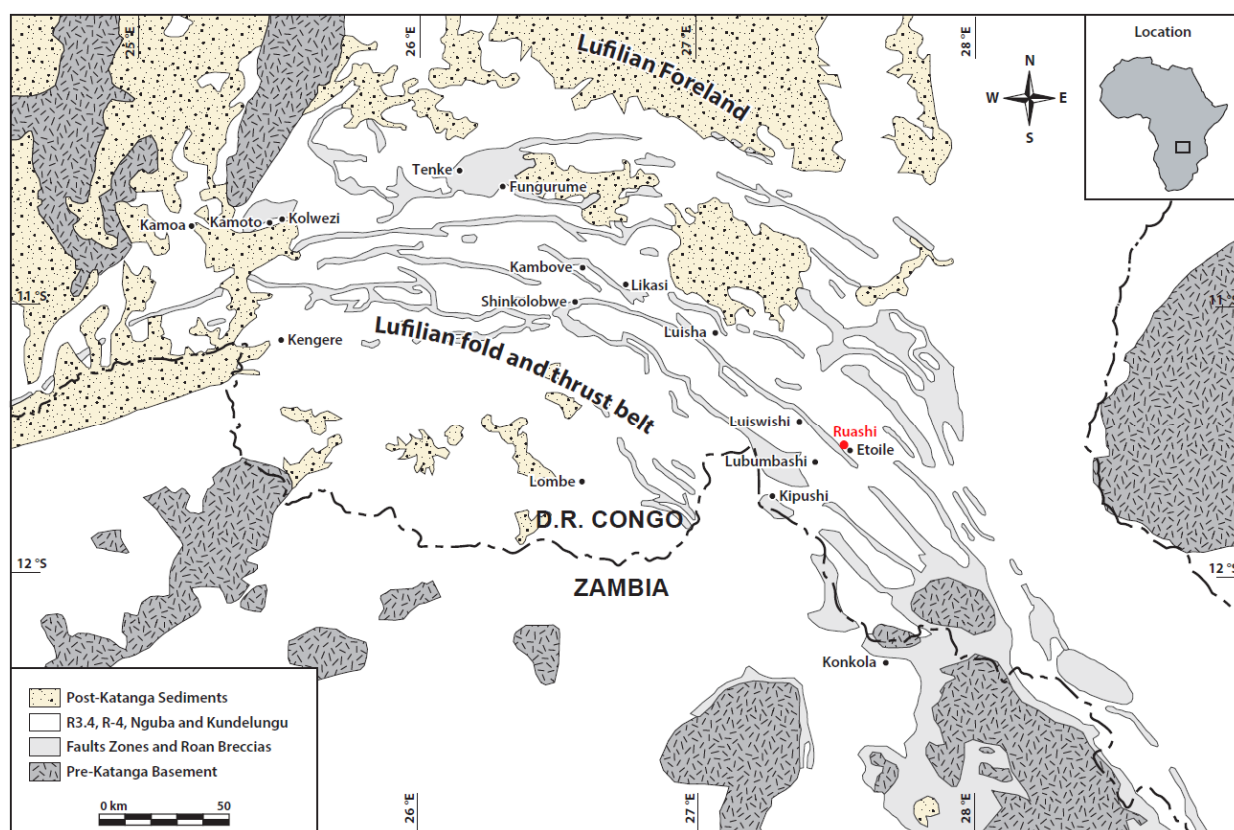


Figure 1. Geological map of the Central African Copperbelt with the Katanga Supergroup rocks and location of the Ruashi deposit indicated [18].

The Neoproterozoic Katanga Supergroup has recently been subdivided into four groups, from bottom to top: the Roan, Nguba, Kundelungu and Bianco groups (Figure 2) [19]. The Roan Group consists of a succession of dolostone, shale, mudstone, siltstone, and sandstone that was deposited on a carbonate platform [18,20–22]. According to Batumike et al. [23], the Nguba group is separated from the underlying Roan by the Mwale Formation (~717–660 Ma; equivalent to Sturtian glaciation) and it is overlain by the Kyanadamu Formation (~635–615 Ma; equivalent to Marinoan glaciation), forming the basal formation of the Kundelungu Group. The main lithologies in the Nguba Group are dolostone, sandstone, siltstone, shale and dolomitic shale [20,24]. The Kundelungu and Bianco groups comprise a succession of arkosic sandstone, shale, conglomerate and sedimentary breccia [23,25,26].

The Roan Group, in both the Katanga Copperbelt (KCB) and Zambian Copperbelt (ZCB), hosts the main Cu-Co ore bodies [3,27,28]. Although this Cu-Co mineralization occurs in several formations (e.g., Kambove, Kamoto, Dolomitic Shale and Kansuki formations), the distribution of the Cu versus Co differs in each formation. Cobalt is highly

concentrated in a particular unit of the Kinsevere Formation (former Dolomitic Shale Formation), named the Black Ore Mineralised Zone (BOMZ) corresponding to the Shale Dolomitic 2a (SD2a) unit of the Mines Subgroup in the Roan [2]. This unit is missing in some deposits, as is the case at Kisanfu, Kwatebala and Tenke because of its occurrence as lenses. The fresh BOMZ unit (1 to 16 m of thick) at the Kamoto Cu-Co deposit consists of a stratified and massive dolostone with large dolomite crystals in association with recrystallized quartz [27,29]. A microscopic study of samples collected from the Shinkolobwe, Kamoto and Kilamusembu Cu-Co deposits has shown that this weathered rock is composed mainly of quartz, dolomite and muscovite, and occasionally magnesite and chlorite [30,31]. Pyrite, chalcopyrite, bornite, chalcocite, siegenite and carrollite are usually observed in minor quantities in the weathered rock. At the Ruashi deposit, the BOMZ (2–6 m thick) unit is marked by a poorly stratified and well-recrystallized dolomite, highly weathered at outcrop, by quartz, and traces of albite. In the weathering zone, the BOMZ unit presents similar characteristics to different Cu-Co deposits within the Lufilian arc. This dolostone is intensely weathered into black sandy and clayey dolostone and clays. At the Luiswishi Cu-Co deposit, the BOMZ is enriched in U and Th [32,33]. Additionally, some major elements increase from the fresh rock (e.g., SiO₂: 26.27%, Al₂O₃: 3.5%, Fe₂O₃: 1.56%) to weathered rocks (e.g., SiO₂: 39.49%, Al₂O₃: 7.55%, Fe₂O₃: 28.28%) Fontaine et al. [31]. Heterogenite with minor chalcocite, malachite or chrysocolla are the main supergene minerals in BOMZ.

Recent research conducted on the Cu-Co ores from both the KCB and ZCB have revealed that high-grade Co can be recovered by implementing new flow sheets such as that of Welham et al. [34]. Contrary to the processes currently used at hydrometallurgical plants operating in the KCB for recovering Co [7,35], i.e., through precipitation as inorganic salts (hydroxides or carbonates) using solutions from the sulphuric leaching of the ores or using raffinates from the solvent extraction (SX) of Cu as starting solution, recent studies propose a new process. This process is based on SX and electrowinning (EW) of Cu and Co, with Cyanex as an extractant for selective recovery of Co from pregnant leach solution (PLS). Prior to the recovery of Co, impurities such as Cu, Zn, Fe, Mn and Al are first removed from the PLS using chemical processes [36–38]. The recovery of Co based on traditional hydrometallurgical processing of Cu-Co ores results in hydroxides with grades ranging between 22 and 30%. Therefore, a need exists to invest in a better process to recover the high-grade Co from the BOMZ. This implies testing new processing routes in order to increase the recovery of Co. The outcome of this research will most likely require constructing new sections in operational plants dedicated to the recovery of Co.

In this paper, the Ruashi Cu-Co deposit is used as a case study to: (i) define and compare the main geometallurgical properties (grades, mineralogy, textures) of the BOMZ and CMN ore types, (ii) to better understand these properties on Co recovery and metallurgical behaviour, (iii) to propose a new hydrometallurgical processing route for Co recovery from the BOMZ ore, and (iv) to demonstrate how a detailed geometallurgical assessment of marginal ore types in SHSC deposits could help to enhance cobalt by-product recovery and reduce losses.

2. Geological Background

2.1. Lithostratigraphical Distribution of the Cu-Co Mineralisation

The African Copperbelt comprises south-eastern Congo and northern Zambia. The Cu-Co (U) and Cu (Pb, Zn) mineralization in the Katanga Supergroup is controlled by the lithology and tectonics [2,18,24,27,28,39–41]. Figure 2 shows a lithostratigraphic succession of the Katangan rocks with the Cu-Co mineralization indicated [19,23]. The Roan Group at the base of the Katanga Supergroup hosts the major stratiform to stratabound Cu-Co (U) deposits [42–44]. The Cu-Co deposits in the KCB are situated in the Mines Subgroup (e.g., at Etoile, Tenke-Fungurume, Kamoto, Kambove, Luiswishi and Ruashi) and in the Kansuki Formation (e.g., Shituru and Kipoï deposits). In the ZCB, Cu-Co mineralization occurs in the Mindola and Kitwe formations and the Mwashia Subgroup of the Roan Group [3,45]. In the overlying Nguba and Kundelungu groups in both the KCB and ZCB,

stratiform to stratabound Co-rich deposits are absent. However, they do host either Cu mineralization (e.g., Fisthie, Kamoia, Kakula and Shangoluwe deposits; [26,46–50]) or Cu (Pb, Zn) mineralisation (e.g., Kipushi and Dikulushi deposits; [51–54]).

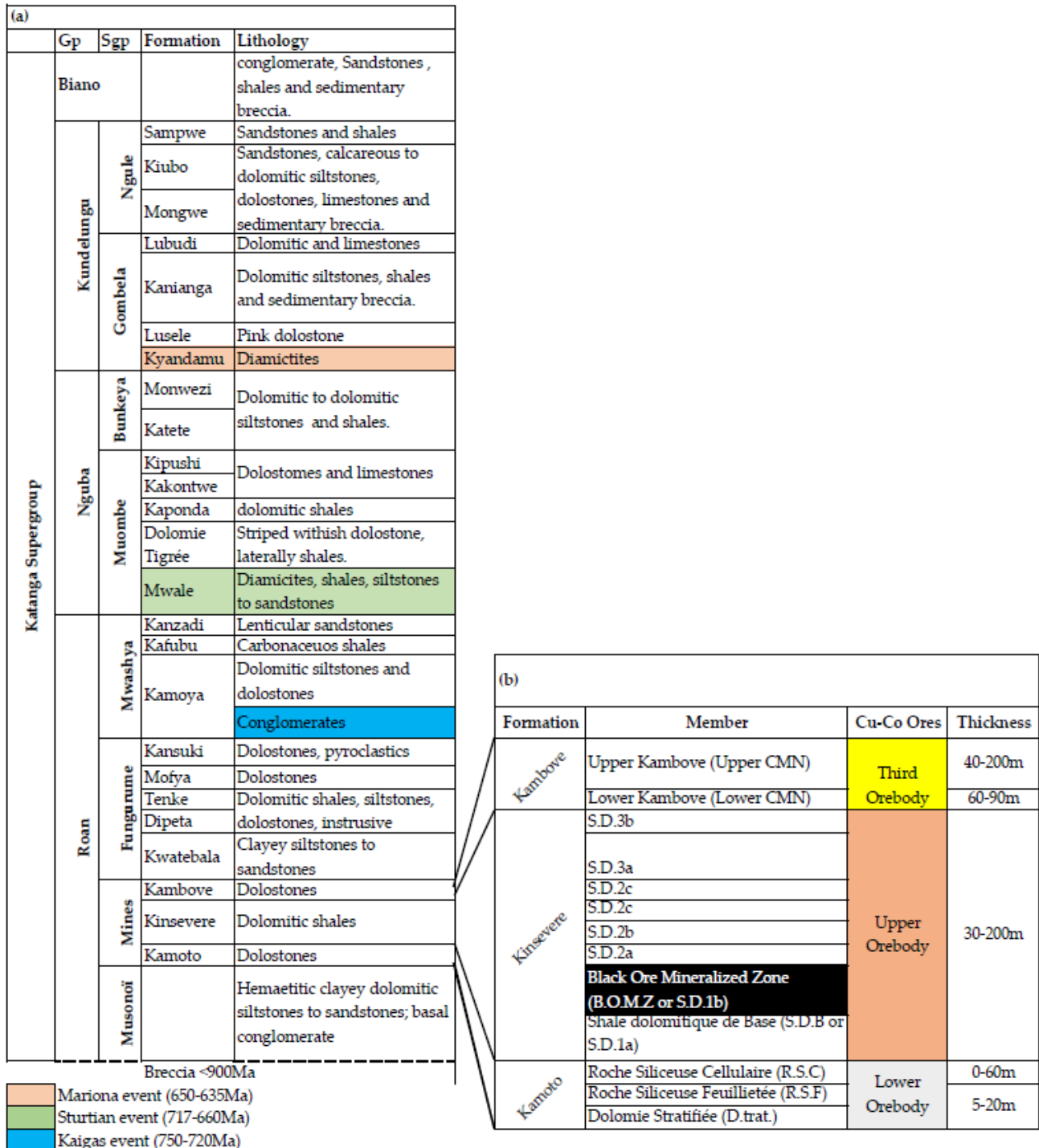


Figure 2. (a) Lithostratigraphy of the Katanga Supergroup from Batumike et al. [23] modified by Cailteux and De Putter [19]. Glaciation intervals are marked by the Kaigas (~750–720 Ma), Sturtian (717–660 Ma), and Marinoan (~650–635 Ma) glaciations. Ages are from Master et al. [25], Key et al. [55], Barron et al. [56], Rooney et al. [57]. Definition of sedimentary breccia and subdivision of the Kamoya Formation respectively by Mambwe et al. [22,58]. (b) Lithostratigraphy subdivision of the Mines Subgroup within the Cu-Co ores bodies.

2.2. Geology of Ruashi Cu-Co Deposit

The Ruashi Cu-Co ore deposit is located ~7 km NE of the city centre of Lubumbashi in the DR Congo. The deposit consists of three distinct mega breccias of the Mines Subgroup named Ruashi I, II and III (Figure 3). They occur along the NW-SE Etoile-Luiswishi alignment [59]. The Ruashi deposit contains around 45.8 Mt ores at a grade of 2.81% Cu and 0.246% Co [60]. Presently, the Ruashi Mine produces around 440 t of Co and 38,000 t of Cu per year. The Union Minière du Haut-Katanga (UMHK) discovered the Etoile (Star of Congo Mine) and Ruashi Cu-Co deposits in 1911. In 1920, the same mining company developed the open pit at the Ruashi ore body I and extracted the oxidized ores malachite and chrysocolla. In 1967, the UMHK was nationalized by the central government and renamed “Gécamines”. As a consequence of the privatization of the mines in 1997, several new projects were evaluated at the Ruashi mine, such as the exploitation of the stockpiles by the Cobalt Metals Company. Since 2007, mining operations were restarted by Ruashi Mining, owned by the Metorex group, and later by Jinchuan International [61], all in partnership with Gécamines.

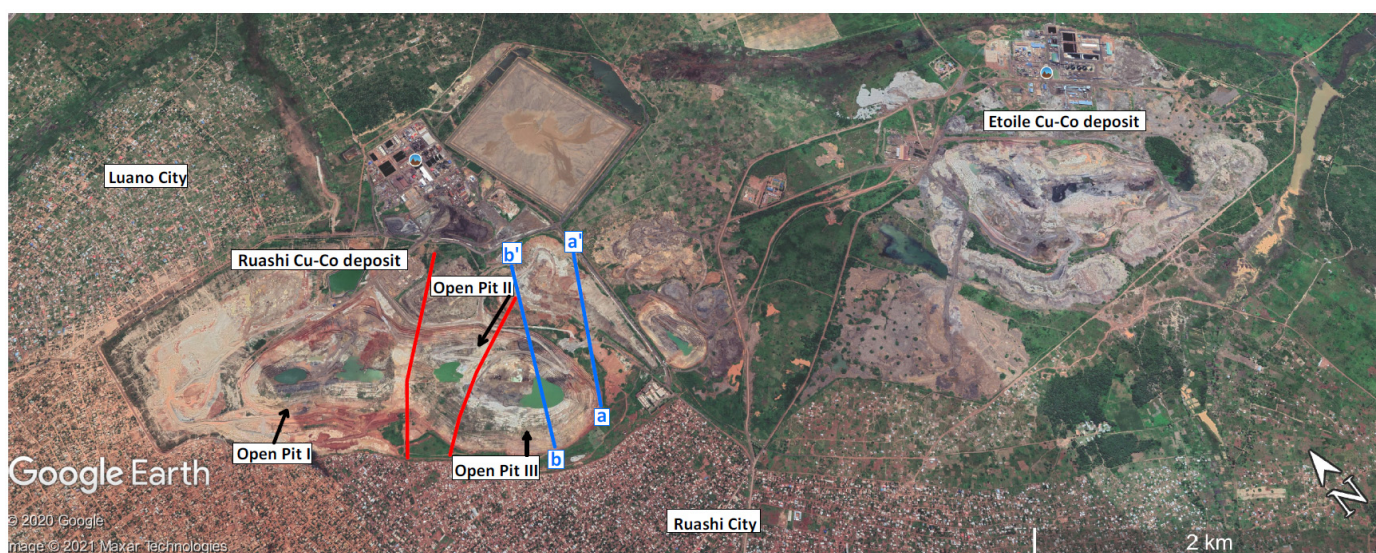


Figure 3. Location of the Ruashi Cu-Co deposits on the Google Earth map, west to the Etoile Cu-Co deposit. aa' and bb' are cross-sections in the eastern part of the Ruashi III (open pit III). Two faults (in red) form the boundary between the three open pits at Ruashi.

The Ruashi I deposit is the largest of the three. It is located to the north-west of the Ruashi II deposit and extends over a length of ~900 m and a width of 350 m. It is characterized by a large oxidized zone that reaches a depth of ~130 m below the surface, whilst only hypogene sulphide mineralization has been intersected at a depth of >300 m. The orebody is terminated by a brecciated shear zone on both its north-western and south-eastern margins (Figures 4 and 5). Ruashi II is a smaller deposit with a length of ~200 m and a width of ~250 m. It lies in the middle between the Ruashi I and III deposits. The Ruashi III deposit is ~650 m long and >200 m wide. All three deposits are intensively fractured and overly Kundelungu Group rocks. The contact with the latter is formed by a polymict breccia. The Fungurume Subgroup (former Dipeta Subgroup) within the Roan consists of stratified grey dolostone, silty grey dolostone and grey whitish and talcaeous dolostone with crocidolite (white riebeckite). These rocks separate the Mines Subgroup from the Kundelungu rocks in the southern part of the deposits.

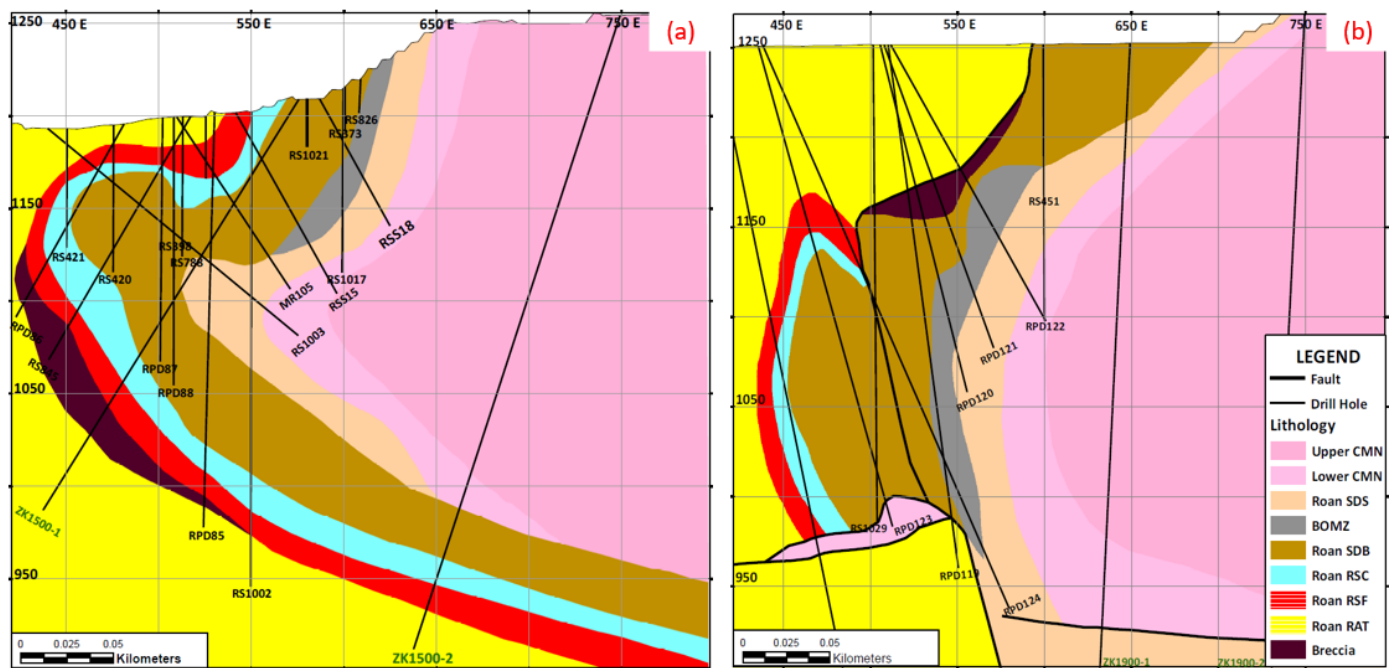


Figure 4. Geological structure of the Ruashi deposit (a) and (b) Cross sections oriented north-east to south-west, showing the lithostratigraphic succession of the Mines Subgroup with the RAT, RSF, RSC, SDB, BOMZ, SDS and the Lower and Upper CMN.

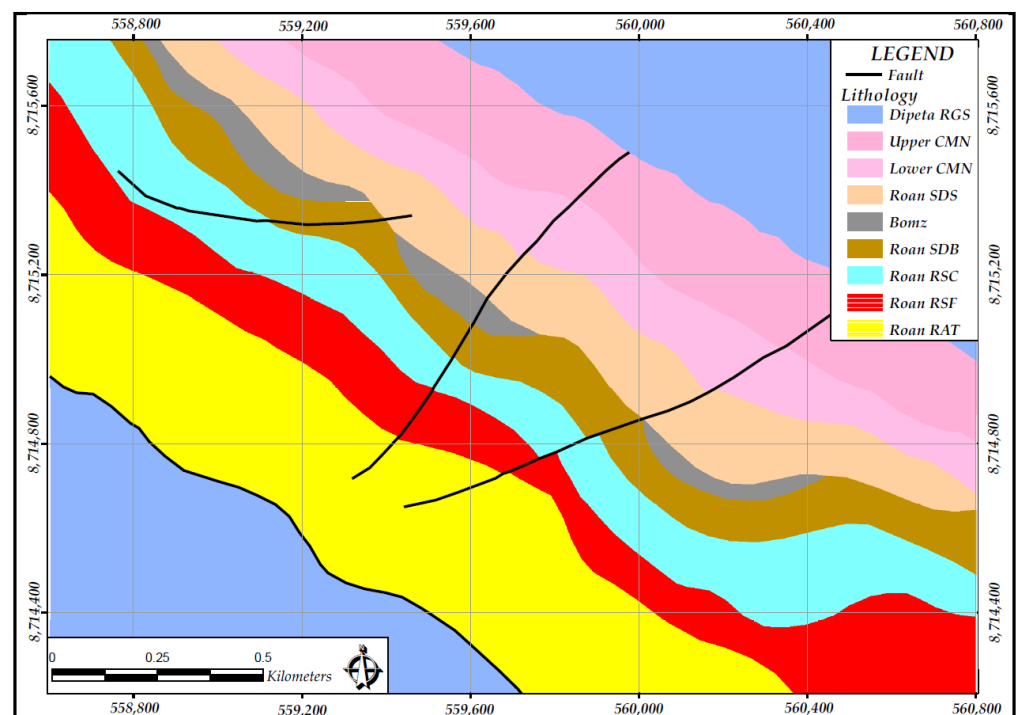


Figure 5. Geological map of level 1280 m at the Ruashi deposit. The BOMZ unit is present as lenses. Strike slip faults separate the Ruashi I (open pit I), II (open pit II) and III (open pit III).

The lithostratigraphic succession and the associated Cu-Co mineralization at Ruashi are typical for those described in the Mines and Musonoï subgroups along the Lufilian arc such as at Luiswishi, Tenke-Fungurume, Kambove, Kolwezi and Luisha [18,44,62,63]. The Musonoï Subgroup or the former RAT Subgroup is overlain by the Mines Subgroup, comprising from bottom to top, the Kamoto (Roche Siliceuse Cellulaire, Roche Siliceuse

cyclones. The overflow (OF) of cyclones constitutes the feed to the pre-leaching section whereas the cyclones underflow (UF) is returned back to comminution inside Ball Mills working in closed circuit with cyclones [61]. As a result, a pulp composed of 70–75% of solid particles smaller than 74 μm is obtained and subjected to thickening (using 20% Bronte 103 as flocculent) so that its specific gravity is raised from 1250 up to 1550–1600 kg/m^3 . The sulphuric acid (pH: 1.5–1.8) leaching of comminuted ores (pulp) is conducted over 8 h inside four agitated reactors (two hours in each) under reducing conditions (2 g/L $\text{Na}_2\text{S}_2\text{O}_5$ or a Redox potential of 425–450 mV). The leaching of ores enables a high-grade (7–10 g/L Cu) pregnant leach solution (PLS) to be obtained, with the solid residues scavenged for valuable metals through washing inside the counter-current decanters (CCDs). This scavenging process produces a low-grade (5–6 g/L Cu) PLS. The high-grade PLS undergoes SX of Cu using an organic phase composed of LIX 984N as extractant (10–33%) diluted in Sasol 210 (67–90%) as solvent prior to EW of Cu in view of producing commercial-grade cathodes (99.99%). As for the low-grade PLS, it undergoes purification through chemical precipitation of Fe, Al and Mn followed by the recovery of Co [7] which is precipitated as hydroxides (22–30%). The precipitating reagent of cobalt consists of a mixture of MgO and NaOH (pH: 7.5–8.5).

4. Materials and Methods

4.1. Geological Fieldwork, Sample Preparation and Chemical Analysis

The fieldwork focused on mapping at a 1/2000 scale and producing a lithological description of each unit of the Mines Subgroup including the style of mineralization at the Ruashi ore deposit. This step was followed by core logging of 10 boreholes (100 to 300 m total depth) drilled along different transects. Representative samples were collected systematically at the outcrop of the BOMZ and at the base of CMN both within the weathering zone and a mesh of 2.5 m by 5 m at different levels. Each sample was collected from a small sampling grid of 1 m square and 50 cm depth, then mixed and homogenized using a splitter. Twenty-five samples from the BOMZ were collected in open pit III at 1155 m, 1165 m, 1170 m, 1175 m and 1190 m levels. Fifteen samples were collected from open pit I at 1245 m, 1250 m, 1255 m and 1265 m levels and thirty samples from open pit III at 1180 m, 1185 m, 1190 m, 1200 m, 1205 m and 1210 m levels. Sample weights ranged between 2 and 5 kg, and each sample was submitted for thin and polished sections and for a chemical assay by ICP-MS, for major and trace element determinations (25 samples of BOMZ and 55 samples of Lower CMN). We used the IOGAS software to interpret the geochemical data. The standard diagrams of Terry and Chillingar [65] were used for the determination of the modal composition of the minerals in the thin section under the microscope.

Additionally, a 50 kg composite sample of the BOMZ from Ruashi open pit III was prepared through mixing and homogenization. The composite sample was fragmented using a 100 mm \times 130 mm 911MPE-JC100 Model Jaw crusher, with the discharge passing over a 2.3 mm aperture sieve and re-crushing of the oversize. Subsequently, four subsamples of 1 kg each of the undersize were prepared using a rifle sampler. Aliquots (2 g) were finely fragmented using a vibrator grinder, with 0.5 g of the material dissolved, in duplicate, using aqua regia (5 mL concentrated nitric acid and 10 mL concentrated hydrochloric acid). The obtained solution was heated, boiled for 1 min in view of a complete digestion and subsequently diluted (5 mL in 250 mL of distilled water) prior to spectrophotometric analyses of Cu (0.41%), Co (1.21%), Fe (3.52%) and Mn (0.95%) using an AAS 300 Analytik Jena spectrophotometer (Analytik Jena, Jena, Germany) equipped with Kinesis hollow cathode lamps (multi-element in standard 1 $\frac{1}{2}$ " (37 mm)).

4.2. Grindability of the BOMZ Sample

One kg of crushed BOMZ (from Ruashi open pit III) with a particle size smaller than 2.3 mm, was subjected to wet grinding inside a lab rod mill (152 mm inside diameter \times 305 mm length, containing 10 7 kg steel rods with 19 mm diameter \times 279 mm length and one litre of tap water) operated at 70 rpm while varying the grinding time as follows: 3, 6, 9, 12 and

15 min. The grinder discharge was screened using a 212 μm aperture sieve. The oversize was washed, dried at 107 $^{\circ}\text{C}$ for 48 h in a Memmert steam room before being weighted using a Mettler Toledo SB 1600 analytic balance. The proportion of oversize was plotted versus the grinding time (Figure 7). The wet grinding of BOMZ rocks for 11 min was considered as optimal considering that it enabled obtaining 25% of the oversize from a 212 μm aperture sieve.

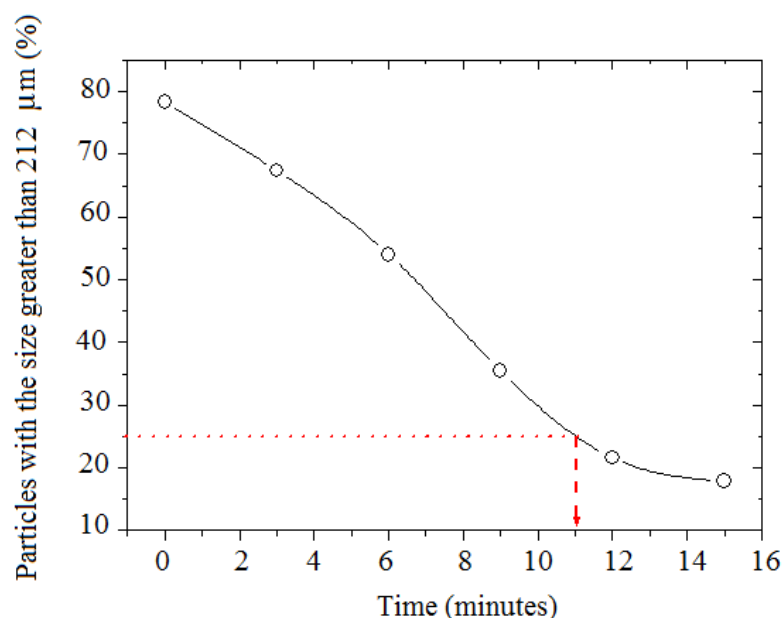


Figure 7. Grindability curve of BOMZ rocks.

4.3. Sulphuric Acid Leaching of BOMZ

Leaching tests of BOMZ rocks were achieved in duplicate through magnetic stirring (Fischer Scientific magnetic stirrer) at a constant speed (500 rpm), in aqueous sulphuric acid over 8 h, under reducing conditions. A pulp with particle size smaller than 212 μm and a specific gravity of 1500 kg/m^3 (1.17 kg of solid particles in a mixture with one litre of an aqueous solution of sulphuric acid (30 g/L) and 2.5 g/L of SMBS (300–350 mV) was prepared. The aqueous solution was prepared using analytical-grade reagents: SMBS ($\geq 98.0\%$) provided by WVR Chemicals and concentrated sulphuric acid (98.0%) from MERCK. The redox potential (versus SHE at 25 $^{\circ}\text{C}$) was measured using a CONSORT C933 analyser and a Sen Tix ORP (WTW) electrode. The pulp pH was adjusted between 1.6 and 1.8 using the same analyser and an SP10B general-purpose electrode coupled with an ATC (Pt 1000) electrode. At every 30-min interval, 5 mL of pulp was collected, vacuum filtered, and the recovered aqueous solution spectrophotometrically assayed for Cu, Co, Fe and Mn (using an SAA 300 Analytik Jena spectrophotometer, Jena, Germany) in view of following up the leaching kinetics of the BOMZ. The results are expressed as yields of metals of interest versus time.

4.4. Leach Liquor Purification by Solvent Extraction

The Cu was removed through SX from the aqueous phase (300 mL) prepared during the sulphuric acid leaching of BOMZ, with the pH varying in the range 1.5–5.0, using analytical-grade chemicals: ACORGA OPT 5510 provided by Cytec Industries Inc. (Seattle, WA, USA), and LIX 984N from BASF, Ludwigshafen, Germany. The organic phase (300 mL), composed of either ACORGA OPT 5510 (20%) or LIX 984N (20%) diluted in paraffin (80%), was mixed with the aqueous phase under magnetic stirring in a 1000 mL beaker over 3 min. The mixture was allowed to settle for 1 min and 30 s in order to separate the organic and aqueous phases. The Cu was transferred to the organic phase and was stripped threefold by means of a fresh electrolyte (sulphuric acid aqueous solution-250 g/L), which was later

spectrophotometrically analysed to determine the recovery yields of Co, Cu, Fe and Mn. The raffinate resulting from the extraction of Cu was subjected to SX of Mn, with the pH varying in the range 1.5–5.0 using analytical-grade chemicals LIX 63 provided by BASF and neodecanoic acid 99.0% provided by Shanghai Jinjinle Industry Co, Ltd., Shanghai, China. The organic phase was composed of two solutions: 65% LIX 63 and 35% Neodecanoic acid (in volume proportions). The two components or solutions were prepared by diluting 20% LIX 63 in 80% xylene and 30% Neodecanoic acid in 70% xylene, respectively.

4.5. Precipitation of Cobalt as Hydroxides

The Co was recovered as hydroxides, from the raffinate given by the SX of Mn, using a mixture of analytical-grade chemicals as precipitating agents: MC40 magnesia (98.0%) provided by Martin Marietta and caustic soda tablets (98.0%) from MERCK prepared as 5 N solution. Different amounts of pure MC40 magnesia, determined based on the ratio MgO/Co, were added to 500 mL of the leach liquor that was allowed to rest for 3 h, followed by the addition of an aqueous solution of NaOH (5 N) until pH adjustment at 8.2. Later on, 10 mL of the flocculent (20% Bronte 103) was added and the mixture subjected to stirring in view of improving the precipitation process of Co. The mixture was left to settle for about an hour, followed by vacuum filtration of the precipitate. The latter was dried at 105 °C, inside a Memmert steam room for 24 h, and subjected to spectrophotometric analysis of Co and other metals of interest, i.e., Cu, Fe and Mn.

5. Results

5.1. Petrography and Ore Mineralogy

The BOMZ unit at Ruashi shows a succession of stratified and massive dolostones. These rocks are intensely weathered to black argillaceous and siliceous dolostones. In the outcrops and cores, supergene ore is mainly presented by malachite and heterogenite locally associated with chrysocolla and spherocobaltite (Figure 8a–c). These supergene minerals are preferentially concentrated in bedding planes, fractures, and dissolution cavities. In thin sections, the clayey dolostone is composed of euhedral dolomite crystals (15 vol.%), magnesite (2 vol.%), authigenic quartz (20 vol.%) and muscovite (13 vol.%). The muscovite is present as white elongated flakes embedded in an authigenic quartz cement. Fine-grained quartz and small dolomite crystals give an equigranular texture to the rock. Polished sections (Figure 8d–f) show a high content of malachite (15 vol.%) and heterogenite (10 vol.%) associated with goethite (15 vol.%), plus a minor amount of hematite (4 vol.%) and black Fe oxides (2 vol.%).

Sulphide minerals are represented by chalcopyrite (1 vol.%), carrollite (1 vol.%), bornite (1 vol.%), pyrite (1 vol.%) and chalcocite (5 vol.%). Carrollite (5 vol.%) is usually disseminated in the dolomite cement while chalcopyrite together with bornite replace pyrite. Malachite replaces chalcopyrite from the periphery towards the centre of mineral. In certain samples, coarse-grained chalcocite, bornite and chalcopyrite float within authigenic quartz and carbonate cement. In quartz and dolomite veins, carrollite is associated with oxide minerals (goethite) in voids and dissolution cavities.

The Lower CMN unit comprises stratified to finely laminated dolostones, which are weathered to clayey and siliceous dolostones. In outcrops exposed in open pits and in the cores, the rock is red to black and is mineralized with malachite, chrysocolla and heterogenite (Figure 8g–i). In thin and polished sections, the laminated dolostone is composed of a succession of fine- and coarse-grained thin layers (1 to 2 mm) consisting of muscovite flakes (10 vol.%), authigenic quartz (20 vol.%) and dolomite (30 vol.%). Fine-grained detrital quartz and authigenic quartz are more abundant than dolomite in the siliceous micro-layers. Hematite (2 vol.%) and goethite (8 vol.%) are commonly present in the authigenic quartz and are associated with malachite (10 vol.%) and heterogenite (3 vol.%).

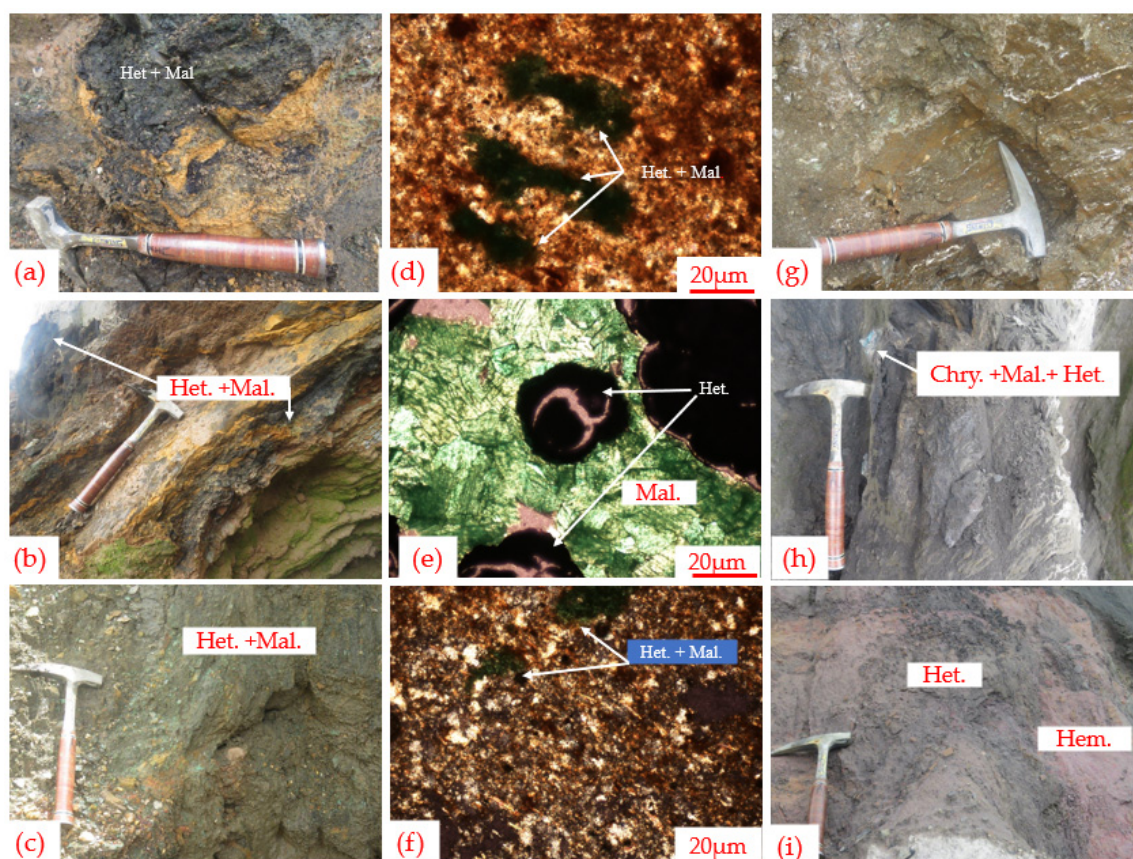


Figure 8. Host-rock petrography and Cu-Co mineralization: (a–c) facies of the BOMZ; (d–f) thin polished sections of the BOMZ showing the mineralization of malachite (Mal.) and heterogenite (Het.); (g–i) facies of the Lower CMN unit with mineralization of chrysocolla (Chry.) malachite (Mal.) and heterogenite (Het.).

The iron oxi-hydroxides mentioned above replace pyrite, chalcocopyrite and bornite. Malachite (5%), chrysocolla (3 vol.%) and heterogenite (3 vol.%) fill fractures and cleavage planes. Pyrite (1 vol.%), chalcocopyrite (3 vol.%), carrollite (4 vol.%) and bornite (1 vol.%) are also found in fractures or occur disseminated in the carbonate cement. Chalcocite (2 vol.%) locally replaces chalcocopyrite and is rimmed by hematite. Chalcocite and bornite seem to be more abundant in the Lower CMN than in the BOMZ in the Ruashi ore deposit. The black clay consists of a mixture of fine- to coarse-grained quartz (10 vol.%), dolomite (10 vol.%), malachite (5 vol.%), heterogenite (3 vol.%), pyrite (2 vol.%), carrollite (1 vol.%), chalcocopyrite (2 vol.%) and bornite (1 vol.%). These are embedded in an association of phyllosilicate minerals (e.g., muscovite, chlorite) and authigenic quartz (62 vol.%) and are associated with goethite, hematite, and other Fe oxides (4 vol.%).

5.2. Lithogeochemistry

The distribution of major and trace elements in the BOMZ and Lower CMN differs between each deposit at Ruashi Mining (Figures 9 and 10). In the Lower CMN, SiO₂ (35.67–75.49%) has a higher content than in the BOMZ (12.12–58.75% of SiO₂). The range in the MgO content is slightly higher in the BOMZ (2.43–16.07%) than in the Lower CMN (0.13–15.63%). CaO content is low in the Lower CMN (0.28 and 13.07%) from open pit I and III. The highest aluminium content (Al₂O₃ ≤ 3.74%) is found in the Lower CMN from open pit I, which is characterized by abundant muscovite and chlorite. The BOMZ and Lower CMN units contain Fe₂O₃ (4.99–14.97%) due to the occurrence of hematite and goethite as well as other Fe-Mn oxides associated with the Cu-Co ores. At the Ruashi deposits, the BOMZ contains more Cu and Co than the Lower CMN although they have a similar

mineral paragenesis. In open pit I, the concentration of Co is low (<0.64%). Although the contents of the elements Zr, Ni, Bi, V, Cr, Th, U, Sc, Bi, Nb, Rb, As and Mn, is low, they do show distribution trends (Figure 9b). Figure 9e indicates that the BOMZ and Lower CMN contain more Ni than Pb and Zn. Ba is present at a higher content than Sr, V, Nb, As and Y. Ba has been reported from silicates such as muscovite in Kipushi Zn-Pb-Cu deposits [51].

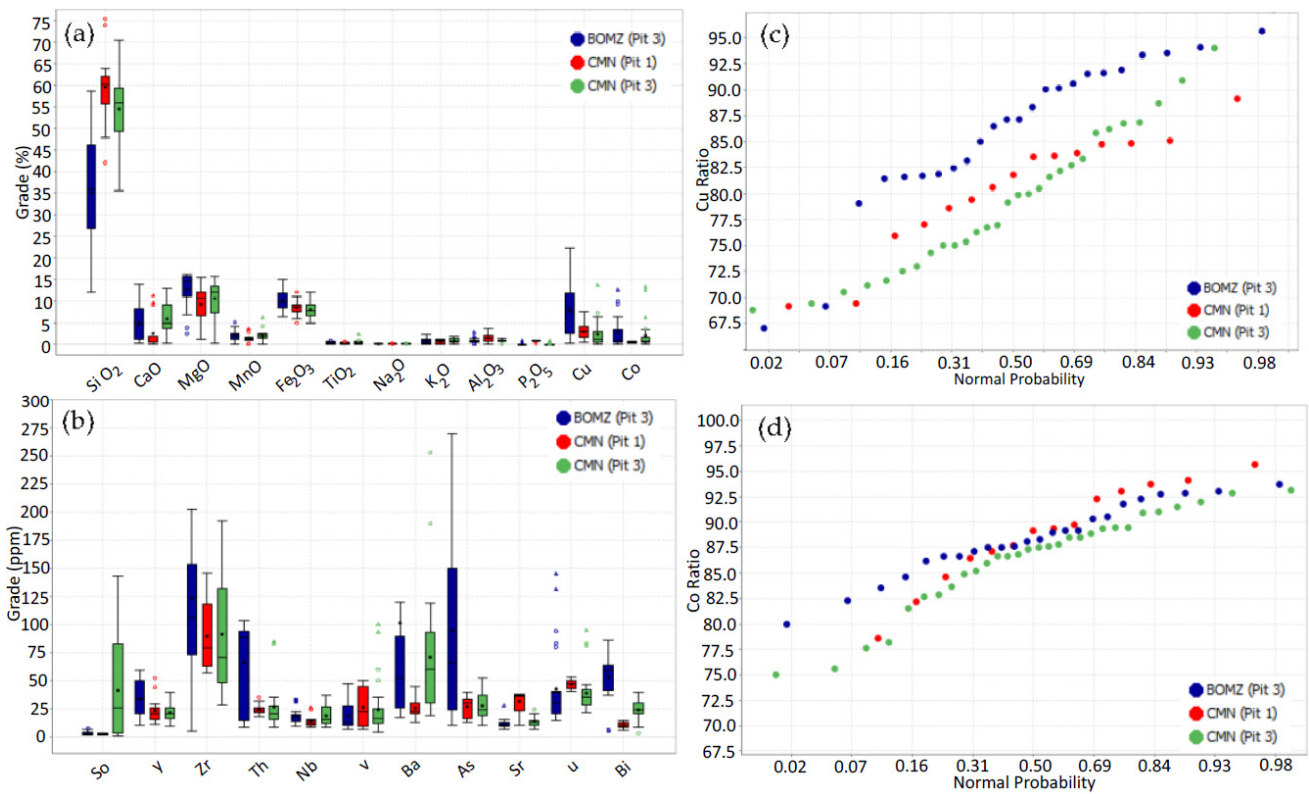


Figure 9. Geochemistry of the BOMZ and CMN: (a) Whisker diagram of the major elements and of Cu and Co; (b) Whisker diagram of the most abundant trace elements; (c,d) Probability plot of the Cu and Co ratio.

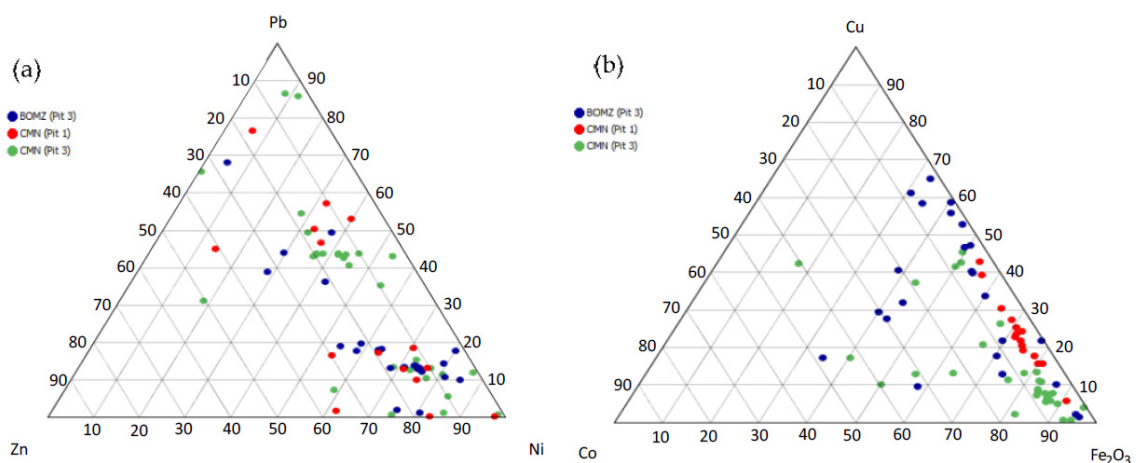


Figure 10. (a) Triangular diagram of Pb-Zn-Ni and (b) Triangular diagram of Cu-Co-Fe₂O₃.

The distribution of Cu and Co reflects the proportion of sulphide and supergene ores in the host rocks. Arsenic could be contained in pyrite and chalcopyrite [66]. Calculated Cu ratio ($100 \times \text{Acid Soluble Cu} / \text{TCu}$), in which TCu is the total Cu, ranges between 69.15% and 95.6% for the BOMZ, and between 69.18% and 94.04% for the Lower CMN. In the

BOMZ, Co ratio ($100 \times \text{Acid Soluble Co} / \text{Total Co}$) varies between 80 and 93% and between 64.41 and 95.65% in Lower CMN. In these two cases, the analysed AS Cu and AS Co are obtained after 4 h of Cu-Co ores leaching in sulphuric acid according to the Ruashi Mining chemistry protocol. The behaviour of the Cu ratio merits more attention because it allows classification of ore types into an oxide, oxide-dominant mixed, sulphide-dominant mixed or sulphide ore subtype. The ore types in Cu-Co deposits are usually determined by the relationship between the Quick Leach Test (QLT), the Cu and Co ratio, and the ore mineralogy. Although the QLT has not been performed, the behaviour of the Cu ratio and the mineralogical assemblage allows the classification of ores in the BOMZ and Lower CMN as oxide ores (Cu ratio $\geq 75\%$) and as oxide dominant mixed ores (Cu ratio $< 75\%$, more chalcocite present in this ore). The abundance of chalcocite in the mixed ores could be due to the supergene origin of this sulphide as described in other Cu deposits [67]. The oxide dominant mixed ores contain unweathered dolostone fragments (millimetre to metric size) with sulphides. The Cu and Co ratio is also influenced by the presence of small amounts of chalcopyrite, bornite, chalcocite and carrollite in both the oxide and oxide-rich mixed ores. The insolubility of the sulphides during the hydrometallurgical processing increased the Cu (up 3%) and Co (up 1%) in the tailing material at Ruashi Mining [59]. Therefore, these tailings form a second source of both Cu and Co for future mine development [68–72].

5.3. Hydrometallurgical Extraction of Cobalt from the BOMZ

This extraction was conducted using a processing scheme based on the sulphuric acid leaching of the BOMZ under reducing conditions, SX of Cu and Mn followed by precipitation of Co in the form of hydroxides.

5.3.1. Sulphuric Acid Leaching of the BOMZ

The leaching of the BOMZ led to the results shown in Figure 11 of which the reading reveals that 8 h is the time that enables the highest dissolution of Co, achieving a yield with a value that varies around 93%. The leaching process of Co is accompanied by significant dissolution of Mn (84%) contrarily to Cu for which the highest leaching yield was 40%. Iron was not strongly dissolved during the leaching process of the BOMZ since its highest leaching yield was smaller than 5%. Considering the presence of impurities in the leach liquor, i.e., Cu and Mn also dissolved during the leaching process of the BOMZ, a purification prior to the recovery of Co is necessary.

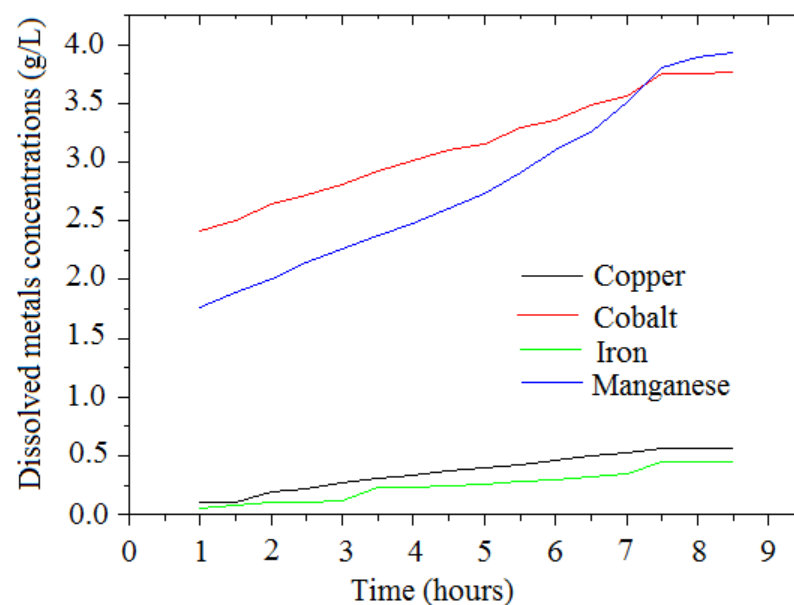


Figure 11. Dissolution kinetics of metals contained in the BOMZ.

5.3.2. Solvent Extraction of Copper

The leach liquor purification through the removal of Cu by SX with ACORGA OPT 5510, was successful in the pH range 1.5–1.8 (Table 1). Indeed, more than 95% Cu was recovered, with the proportion of extracted Co and Mn varying from 0.5 to 1.3% and 0.3 to 0.8%, respectively. The optimal pH for extracting Cu with ACORGA OPT 5510 is 1.7 given that the loss in Co, which is a metal of great interest, was of about 0.5%. However, Fe and Mn were also extracted to yields equal to about 9% and 0.8%, respectively.

Table 1. Leach liquor purification through copper solvent extraction.

pH	Yield of Cu SX with ACORGA OPT 5510 (%)				Yield of Cu SX with LIX 984N (%)			
	Cu	Co	Fe	Mn	Cu	Co	Fe	Mn
1.5	94.70	1.31	9.09	0.80	94.73	1.31	6.81	1.04
1.7	94.69	0.52	9.11	0.79	96.49	0.79	4.54	1.04
1.8	94.68	0.53	9.13	0.29	94.73	0.79	9.09	0.78
2.0	87.61	0.82	2.27	1.01	89.47	1.05	4.54	1.31
3.0	87.64	1.29	2.29	1.02	87.71	1.31	4.54	1.31
4.0	85.92	1.32	4.49	1.57	84.21	1.58	6.81	1.83

During the leach liquor purification by SX using LIX 984N, the highest removal of Cu (96.5%) was achieved when the aqueous phase pH was adjusted to 1.7. Under these conditions, the proportion of co-extracted Co and Mn was lower than 0.8% and 1.5%, respectively. The proportion of Fe removed from the aqueous phase was practically equal to 5%. Above a pH of 1.7 and up to a pH value of 4, the extraction yield of Cu progressively dropped down until it reached a value lower than 85%, with a loss in Co nearing 1.6%. The removal of Mn and Fe reached 6.8% and 1.8%, respectively.

5.3.3. Solvent Extraction of Manganese

The SX of Mn, using the organic phase composed of LIX 63 and Neodecanoic acid, was implemented using the raffinate from the SX of Cu as the starting solution. This enabled the results given in Table 2 to be obtained. The SX of Mn, from the raffinate given by SX of Cu with ACORGA OPT 5510, enabled a yield of about 23% at a pH of 1.7 to be achieved. Under these conditions, more Cu was co-extracted ($\approx 67\%$) with a loss in Co of 2.4%. The highest yield of Mn ($\approx 99\%$) was achieved when the aqueous phase pH was adjusted to 5 and this resulted in a co-extraction of about 27% Co, that is, a loss in Co of 1.6%. Removal of Mn contained in the raffinate given by SX of Cu with LIX 984N, enabled achieving the highest yield (98.1%) when the aqueous phase pH was adjusted to 5. Under such conditions, 25% and 2.8% of Cu and Fe were extracted, respectively.

Table 2. Leach liquor purification through manganese solvent extraction with LIX 63 in synergism with Neodecanoic acid.

pH	Raffinate from Copper SX with ACORGA OPT 5510				Raffinate from Copper SX with LIX 63			
	Cu (%)	Co (%)	Fe (%)	Mn (%)	Cu (%)	Co (%)	Fe (%)	Mn (%)
1.5	33.3	1.9	18.8	22.7	33.3	1.9	4.9	22.5
1.7	66.7	2.4	5.0	23.2	50.0	1.7	4.8	23.3
1.8	58.3	1.6	5.0	25.7	33.3	1.6	2.5	24.4
2.0	57.1	1.9	4.7	22.5	50.0	1.8	4.8	22.8
3.0	57.1	1.3	4.7	20.9	57.1	1.5	2.4	24.7
4.0	37.5	1.6	4.8	47.3	66.7	1.5	4.9	47.5
5.0	27.3	1.6	2.6	98.9	25.0	1.6	2.8	98.1

5.3.4. Recovery of Cobalt as Hydroxides

The precipitation of Co as hydroxides was conducted using the raffinate given by SX of Mn as starting solution, following the removal of Cu either using ACORGA OPT 5510 or LIX 984 N as extractant, with the results obtained given in Table 3. Based on these results, it can be observed that the precipitation of Co with the magnesia, prepared to a [MgO/Co] ratio varying from 0.9 to 1.1, enabled obtaining a cake with a Co grade between 30.0 and 43.5%. Consequently, a yield between 92.0 and 94.5% was achieved, depending on the initial pH of the raffinate resulting from the SX of Cu and Mn and whatever the composition of the organic phase utilized. Moreover, the contents of Mn and Cu in all cakes have remained equal to 0.01% contrary to when the precipitation of cobalt was achieved using a PLS (with the initial pH equal to 1.7) not subjected to SX of Cu and Mn.

Table 3. Precipitate characteristics and yield of cobalt versus the precipitating reagent composition.

Initial PLS pH	MgO (g)	Co (g/L)	Ratio MgO/Co	NaOH-5N Volume (mL)	Final PLS pH	Obtained Cake Weight (g)	Cake Metal Contents (%)				Co Yield (%)
							Cu	Co	Fe	Mn	
4.5	1.71	3.79	0.9	17.8	8.2	5.10 ^A	0.01	40.50	3.45	0.01	94.02
4.5	1.71	3.79	0.9	17.8	8.5	5.10 ^B	0.01	38.90	3.42	0.03	92.50
5.0	1.90	3.78	1.0	17.0	8.2	5.65 ^A	0.01	42.80	3.02	0.01	92.03
5.0	1.90	3.78	1.0	17.0	8.2	5.57 ^B	0.01	40.10	3.00	0.01	92.80
5.5	2.09	3.8	1.1	16.4	8.2	5.99 ^A	0.01	43.30	2.85	0.01	93.90
5.5	2.09	3.80	1.1	16.4	8.2	5.99 ^B	0.01	42.20	2.92	0.01	92.75
1.7	2.28	3.8	1.2	25.3	8.2	5.57 ^C	4.70	30.50	3.79	4.60	89.65

^A Cake obtained using the raffinate from SX of Cu with ACORGA OPT 5510 and SX of Mn with LIX 63 + 10 Versatic acid. ^B Cake obtained using the raffinate from SX of Cu with LIX 984N and SX of Mn with LIX 63 + 10-Versatic acid. ^C Cake from a PLS not subjected to SX of Cu and Mn.

The contents of Cu, Mn and Fe remain as high as 4.70%, 3.79% and 4.60%, respectively, when the PLS not rid of Cu and Mn was subjected to precipitation of Co, with the MgO/Co ratio kept at 1.2. When Cu was eliminated from the leach liquor through SX with AGORGA OPT 5510 and the Mn by SX using LIX 63, together with Neodecanoic acid, the precipitation of Co gave a cake with the highest content of Co (43.3%), that is, with the achievement of a yield of 93.9%, using a PLS with a starting pH of 5.5. In parallel, the precipitation of Co from the raffinate given by the SX of Cu with LIX 984N and the SX of Mn with LIX 63, together with Neodecanoic acid, with a starting pH of 5.5, enabled a cake with the highest content of Co (42.2%), that is, with a yield of 93.75% to be obtained. The Fe content varied in all cakes between 2.8% and 3.5% when Cu and Mn were removed from the PLS through SX.

6. Discussion

6.1. Mineralogical Characteristics of the Host Rock and Distribution of Copper and Cobalt Ores

The Lower CMN is usually present in each deposit, and it is occasionally mineralized as in the case of Kambove West, Ruashi-Etoile and Tenke-Fungurume (e.g., Fungurume 6 and Zikule) deposits. In many deposits in the KCB, this Lower CMN is extensively silicified without any mineralization while the BOMZ is usually missing. The fresh BOMZ is still poorly studied since the Co grade is low in fresh rocks. The alteration of Cu-Co ores in the weathering zone of the Sediment-Hosted Stratiform Copper changes the mineralogy of the gangue and the hypogene ores with depth [43,59,73]. In several major deposits of the KCB (e.g., Etoile, Kanfundwa, Katuto, Luiswishi and Ruashi), a Co cap formed in the uppermost part of the weathering zone. It is mainly composed of heterogenite with minor amounts of other supergene minerals such as malachite and chrysocolla and it occurs associated with Mn-Fe oxides and REE [74,75]. Under the Co cap, there is an enrichment of goethite and hematite, and intense silicification together with the presence of trace amounts

of Cu in the oxidized ores. These characteristics of the Co cap are similar to those described at both the Ruashi and Etoile deposits. This Co cap is missing in other deposits in CACB. In the other deposits, the weathering zones are characterized by a cupriferous ores containing malachite, chrysocolla and pseudomalachite.

The minerals present in the BOMZ and Lower CMN at the Ruashi deposit are the sulphides pyrite, chalcopyrite, carrollite and bornite, and the supergene minerals malachite, chrysocolla and heterogenite. The latter are present along bedding planes, in fractures, in dissolution cavities or occur disseminated in the carbonate cement. The sulphide minerals have not been totally replaced by supergene oxides between the mine levels at 1265 m and 1155 m and the exploitation is in progress towards the mixed zone. The leached zone, usually containing more Fe-oxide, is missing nowadays since it has been mined several years ago. Therefore, the abundance of goethite and hematite at the Ruashi deposit between 1265 m and 1155 m reflects a mineral association with the supergene minerals in the weathering zone. Dolomite, quartz, magnesite, muscovite and chlorite constitute the gangue minerals of the BOMZ and of the weathered Lower CMN. The same gangue mineral association in these two distinct units evidence the same hydrothermal influence in both units. In contrast, talc is an abundant gangue mineral in the weathering zone of the Upper CMN. It probably resulted from the alteration of the dolostone as described in the same unit from the Kambove region by [76]. The absence of talc in the BOMZ and Lower CMN is an advantage because the amount of suspended solids will remain low in an aqueous solution of Cu and Co. In this context, additional flocculants (e.g., Brontë 103) will not be used for the clarification prior to the SX achievement [68,77]. This is an important difference between the ores from the BOMZ and Lower CMN units, and those from the Musonoï Subgroup (cfr. grey and pink RAT) and Kamoto Formation at the Ruashi deposit.

The supergene concentration of Co in the BOMZ and Lower CMN at Ruashi is not so evident as is the case with the immobile and chalcophile elements as Zr, Ni, Bi, V, Cr, Th, U, Sc, Bi, Nb, Rb and As (Figure 9a,b). In the case of the Ruashi deposit as well as for other Sediment-Hosted Stratiform Copper in the KCB, the Cu and Co grades are controlled mainly by the enrichment in supergene minerals (e.g., malachite, heterogenite, chrysocolla and spherocobaltite), with only a minor contribution of sulphide minerals (e.g., chalcopyrite, bornite, carrollite and chalcocite). Five years ago, Co ores mined from the Ruashi deposit contained a very high Co grade (8–16%) and originated from the cobalt cap developed in the subsurface of the deposit. At the level between 1265 m and 1155 m in the Ruashi mine, the oxide ore tonnage and the Co grade decrease, while the proportion of sulphide ores and the Cu grade increases with depth [24,59]. However, a transition zone between the oxide and mixed ores is characterized by the presence of an oxide dominant mixed ore that is influencing the hydrometallurgical processing efficiency in terms of: (i) the recovery of metals of interest as well as their increased retention in the tailings due to the abundant supergene sulphide mineral chalcocite, (ii) the presence of minor amounts of hypogene pyrite, chalcopyrite, bornite and carrollite. The increased presence of sulphide minerals requires a rethink of the in-force mineral processing practices [78].

The trace element distribution at the subsurface along the Lufilian arc is complex [42,74,79]. At the Ruashi deposit, the geochemical anomaly in the BOMZ corresponds to an enrichment of Th, Rb, Y, Cr, As, Zr, Bi, Fe and Ni associated with Cu and Co. At the Mashitu Cu-Co deposit, this geochemical anomaly in the subsurface (30 up to 50 m depth) consists of Co, Bi, V and Mo related to supergene enrichment while Cu, Ni, S and Zn are depleted [80]. A particular case is seen at the Luishia and Luiswishi Cu-Co (U) deposits, where the BOMZ is enriched in Th and U [42,81]. This enrichment is compatible with the presence of primary uranium minerals, i.e., mainly uraninite which is absent at the Ruashi and Mashitu deposits [32,33,82,83]. At the Luiswishi deposit, the BOMZ presents a concentration of both LREE and HREE, while LREE are leached in the other units of the Mines Subgroup in the weathering zone [31,74,84]. This is related to the spatial and temporal distribution of the primary minerals in the Katanga Supergroup. In the weathering zone of both the BOMZ and Lower CMN at the Ruashi deposit, trace and major elements have a similar distribution

since they were affected by the same physico-chemical alteration in the supergene zone and have a similar carbonate host rock. Therefore, the hydrometallurgical processing method proposed for the BOMZ could be extended to the Lower CMN.

6.2. Leaching Kinetics and Extraction of Cobalt

Concerning the leaching behaviour of Co within the BOMZ, the achieved leaching yield is consistent with the lithogeochemical data of the deposit. Indeed, a Co cap exists in the uppermost part of the weathering zone of the deposit. The slowdown observed in the leaching kinetics of Co indicates that Co is also present as a sulphide mineral in the BOMZ. This leaching behaviour of Co, under the implemented leaching conditions, can be explained by its presence as carrollite. Indeed, carrollite is reported in the weathering zone in this study. Besides, the Co leaching yield achieved after four hours of leaching falls within the value range of the AS Co proportion given for the BOMZ from the Ruashi deposit. The greater dissolution of Mn observed during the leaching of BOMZ is related to the presence of black Mn-oxides as well as the possibility of its conversion into a soluble form under reducing conditions.

As for the leaching behaviour of Cu, the achieved yield is lower than the proportion of the AS Cu found in BOMZ from the Ruashi deposit. This behaviour can be well explained by the fact that Cu is present in supergene minerals that are very abundant in the BOMZ. The lower leaching yield is probably due to the conversion of the leached Cu into metal considering that the leaching of the BOMZ was conducted under reducing conditions. Moreover, the Co cap in most deposits of KCB contains less Cu than Co and this also applies to the samples of BOMZ under consideration.

Iron is present in the BOMZ as hematite and goethite as well as black iron oxides. Its lower leaching yield could be due to the presence of pyrite in the BOMZ. It is evident from this and other studies [59,85] that the weathering process of minerals greatly influences the mineralogical composition of the ore in the deposit and ultimately the ore processing technology, especially in terms of the acid consumption and the leaching behaviour of minerals.

Cu is extracted as cathodes from the PLS, resulting from the leaching of Cu-Co ores through the SX and EW, and constitutes the main metal targeted at hydrometallurgical plants operated in the KCB. Given that the Cu grade is lower than that of Co in the BOMZ, Co is the main product targeted in this paper, with Cu recovered as a secondary product. Mn present in the PLS is one of the main impurities which is usually removed using solely chemical-based precipitation processes prior to the recovery of Co. The SX, as implemented in the process proposed, can be used for removing impurities such as manganese from the PLS [36]. However, further studies involving operational and cost aspects need to be considered in view of its applicability at the industrial scale.

After the removal by SX of Cu and Mn, the grades and recovery yields of Co through precipitation are greater than when Co was precipitated using a non-purified PLS. Giving preference to the economy of the reagents MgO and NaOH, the best precipitation conditions for recovering Co contained in the PLS are the ones enabling cakes grading 40.5% Co to be obtained, recovered at a yield of about 94%, and 38.9% Co, recovered at a yield of about 93%, respectively. Mn concentrations in the cake were as low as 0.01% and 0.03%, respectively. During the processing of the BOMZ, Co has been precipitated as high-grade hydroxides from a purified PLS. The enhancement of the grade in the obtained hydroxides results from the use of BOMZ as starting material instead of a blend of Cu-Co oxidized ores traditionally processed at hydrometallurgical plants operated in the KCB [35,86]. This also results from the PLS purification by SX contrary to the widespread practice at hydrometallurgical plants, which rely on the removal of impurities from the low-grade PLS through chemical precipitation (Fe, Al and Mn) prior to the recovery of Co [37,38,87]. The removal of Mn from the PLS through SX enables an enhancement of the quality of the cake of hydroxides given by the precipitation of cobalt as well as minimizing the drop in the process efficiency experienced at Ruashi [88].

7. Conclusions

In the present study, a detailed mineralogical and geochemical analysis is performed in order to understand the efficiency of the hydrometallurgical process of the Black Ore Mineralised Zone in the Katanga Supergroup. From these investigations, it can be concluded that:

- The mineralogy changes from a cobaltiferous ore in the shallow subsurface to a cupriferous ore at deeper zones in both the BOMZ and the Lower CMN. This means that the hydrometallurgical processing of the ores of the shallow subsurface layers of the deposit is of most interest for the extraction of Co whereas the ores from deeper levels are more suitable for the extraction of copper.
- From 1155 m to 1265 m, both the BOMZ and the Lower CMN in the Ruashi mine contain oxide ores with a few local oxide dominant mixed ore packages. Sulphide minerals are more abundant in oxide dominant mixed ore than in the oxide ore and represent relics of unweathered rocks. These relics occur along a fault zone with the latter being intensely mineralized or at the base of the oxidized part of the supergene enrichment zone, which is characterized by relatively high MgO and CaO contents. The hydrometallurgical processing of ores from these parts of the deposit results in an increased retention of the metals of interest in the tailings.
- Talc is absent in the BOMZ and Lower CMN, and the gangue minerals in the weathering zone are still characterized by pyrite, carbonate, quartz, magnesite, chlorite, hematite, and goethite.
- Cu and Co are enriched in the weathering zone, where they are associated with the immobile elements Th, Rb, Y, Cr, As, Zr, Bi and Ni. This geochemical Cu and Co anomaly could be used in mineral exploration of base metals in the Katanga Copperbelt. The cobalt concentration in the BOMZ and the Lower CMN is directly related to the abundance of heterogenite and to a minor extent to carrollite.
- The processing of the BOMZ mined from the Ruashi deposit, using a new method, enables recovery of Co with a high yield as hydroxides, with an enhanced grade in Co. The recovery is larger than the ones achieved at hydrometallurgical plants using Cu-Co ores as feed and applying chemical precipitation for ridding the pregnant leach solution of impurities.

Author Contributions: Conceptualization, P.M. (Pascal Mambwe) and M.S.; methodology, P.M. (Pascal Mambwe) and M.S.; software, P.M. (Pascal Mambwe); validation and formal analysis, M.C., M.S., P.M. (Philippe Muchez), P.M. (Pascal Mambwe) and T.K., investigation and resources, M.C., T.K., M.S. and P.M. (Pascal Mambwe); data curation, P.M. (Pascal Mambwe), P.M. (Philippe Muchez) and M.S.; writing—original draft preparation, P.M. (Pascal Mambwe), M.C. and M.S.; writing—review and editing, P.M. (Pascal Mambwe), M.C., P.M. (Philippe Muchez) and M.S.; visualization, P.M. (Pascal Mambwe) and M.S.; supervision, M.C., P.M. (Philippe Muchez) and M.S.; project administration, M.S. All authors have read and agreed to the published version of the manuscript.

Funding: This research received no external funding.

Data Availability Statement: Not applicable.

Acknowledgments: Pascal Mambwe and Philippe Muchez are member of SIM²-KU Leuven Institute for Sustainable Metals and Minerals. Authors thank Ruashi Mining SA for access and permission to publish the results of this research. Stephane Bila and Geologists from Ruashi Mining SA are thanked for the stimulating discussions. Thanks to Guofeng Liu and Fiston Kabo for the GIS and geological software support and Saffy Thorn for checking the English spelling. The comments of Quentin Dehaine and three anonymous reviewers were extremely helpful and are appreciated.

Conflicts of Interest: The authors declare no conflict of interest.

References

1. Katekesha, F.; Bartholome, P.; Ruiz, J.L. Cobalt zoning in microscopic pyrite from Kamoto, Republic of the Congo (Kinshasa). *Miner. Depos.* **1971**, *6*, 167–176.
2. Cailteux, J.; Kampunzu, A.; Lerouge, C.; Kaputo, A.; Milesi, J. Genesis of sediment-hosted stratiform copper–cobalt deposits, central African Copperbelt. *J. Afr. Earth Sci.* **2005**, *42*, 134–158. [[CrossRef](#)]
3. Selley, D.; Broughton, D.; Scott, R.; Hitzman, M.; Bull, S.; Large, R.; McGolrick, P.; Croaker, M.; Pollington, N.; Barra, F. A new look at the geology of the Zambian Copperbelt. In *Economic Geology: One Hundredth Anniversary Volume, 1905–2005*; Hedenquidt, J.W., Thompson, J.F.H., Goldfarb, R.J., Richards, J.P., Eds.; Society of Economic Geologists: Littleton, CO, USA, 2005; pp. 965–1000.
4. Muchez, P.; Andre-Mayer, A.S.; El Desouky, A.H.; Reisberg, L. Diagenetic origin of the stratiform Cu-Co deposit at Kamoto in the central African Copperbelt. *Miner. Depos.* **2015**, *50*, 437–447. [[CrossRef](#)]
5. Muchez, P.; André-Mayer, A.-S.; Dewaele, S.; Large, R. Discussion: Age of the Zambian Copperbelt. *Miner. Depos.* **2017**, *52*, 1269–1271. [[CrossRef](#)]
6. Slack, J.F.; Kimball, B.E.; Shedd, K.B. Cobalt. *Critical Mineral Resources of the United States—Economic and Environmental Geology and Prospects for Future Supply*; Schulz, K.J., DeYoung, J.H., Seal, R.R., Bradley, D.C., Eds.; U.S. Geological Survey: Reston, VA, USA, 2017; p. 797. [[CrossRef](#)]
7. Sole, K.C.; Parker, J.; Cole, P.M.; Mooiman, M.B. Flowsheet options for cobalt recovery in African copper-cobalt hydrometallurgy circuits. *Miner. Process. Extr. Metal. Rev.* **2019**, *40*, 194–206. [[CrossRef](#)]
8. Dehaine, Q.; Tijsseling, L.T.; Glass, H.J.; Törmänen, T.; Butcher, A.R. Geometallurgy of cobalt ores: A review. *Miner. Eng.* **2021**, *160*, 106656. [[CrossRef](#)]
9. Crundwell, F.K.; Moats, M.S.; Ramachandran, V.; Robinson, T.G.; Davenport, W.G. *Extractive Metallurgy of Nickel, Cobalt, and Platinum-Group Metals*; Elsevier: Oxford, UK, 2011; p. 610.
10. Crundwell, F.K.; Du Preez, N.B.; Knights, B.D.H. Production of Cobalt from Cu-Co ores on the African Copperbelt—An overview. *Miner. Eng.* **2020**, *156*, 106450. [[CrossRef](#)]
11. Leshner, C.M.; Keays, R.R. Komatiite-associated Ni-Cu-PGE deposits: Geology, mineralogy, geochemistry, and genesis. In *The Geology, Geochemistry, Mineralogy and Mineral Beneficiation of the Platinum-Group Elements*; Cabri, L., Ed.; Canadian Institute Mineral Metallurgy Petroleum: Montreal, QC, Canada, 2002; pp. 579–618.
12. Gleeson, S.; Butt, C.; Elias, M. Nickel Laterites: A Review. *SEG Discov.* **2003**, *54*, 11–18. [[CrossRef](#)]
13. Jébrak, M.; Marcoux, E. *Géologie des Ressources Minérales*, 1st ed.; Ministère des Ressources Naturelles et de la Faune: Montreal, QC, Canada, 2008; p. 667.
14. Dehaine, Q.; Michaux, S.P.; Pokki, J.; Kivinen, M.; Butcher, A.R. Battery minerals from Finland: Improving the supply chain for the EU battery industry using a geometallurgical approach. *EGJ* **2020**, *49*, 5–11.
15. Takahashi, V.C.I.; Junior, B.A.B.; Espinosa, D.C.R.; Tenório, J.A.S. Enhancing Co recovery from Li-ion batteries using grinding treatment prior to the leaching and solvent extraction process. *J. Environ. Chem. Eng.* **2020**, *8*, 103801. [[CrossRef](#)]
16. Xu, P.; Tan, D.H.; Chen, Z. Emerging trends in sustainable battery chemistries. *Trends Chem.* **2021**, *3*, 620–630. [[CrossRef](#)]
17. Mbuya, B.; Ntakamushi, P.; Kime, M.-B.; Zeka, L.; Nkulu, G.; Mwamba, A.; Mulaba-Bafubandi, A.F. Metallurgical Evaluation of the Leaching Behavior of Copper–Cobalt-bearing Ores by the Principal Component Analysis Approach: Case Study of the DRC Copperbelt Ore Deposits. *J. Sustain. Met.* **2021**, *7*, 985–994. [[CrossRef](#)]
18. Cailteux, J. Lithostratigraphy of the Neoproterozoic Shaba-type (Zaire) Roan Supergroup and metallogenesis of associated stratiform mineralization. *J. Afr. Earth Sci.* **1994**, *19*, 279–301. [[CrossRef](#)]
19. Cailteux, J.L.H.; De Putter, T. The Neoproterozoic Katanga Supergroup (D.R. Congo): State-of-the-art and revisions of the lithostratigraphy, sedimentary basin and geodynamic evolution. *J. Afr. Earth Sci.* **2019**, *150*, 522–531. [[CrossRef](#)]
20. Batumike, J.M.; Kampunzu, A.B.; Cailteux, J.H. Petrology and geochemistry of the Neoproterozoic and Nguba Kundelungu groups, Katanga supergroup, southeast Congo: Implication for provenance and geotectonic setting paleoweathering. *J. Afr. Earth Sci.* **2006**, *44*, 97–115. [[CrossRef](#)]
21. Mambwe, M.P.; Lavoie, S.; Delvaux, D.; Batumike, J.M. Soft sediment deformation structures in the Neoproterozoic Kansuki formation (Katanga Supergroup, Democratic Republic of the Congo): Evidence for deposition in a tectonically active carbonate platform. *J. Afr. Earth Sci.* **2019**, *150*, 86–95. [[CrossRef](#)]
22. Mambwe, P.; Delpomdor, F.; Lavoie, S.; Mukonki, P.; Batumike, J.; Muchez, P. Sedimentary evolution and stratigraphy of the ~765–740 ma Kansuki-Mwashya platform succession in the Tenke-Fungurume Mining district, Democratic Republic of the Congo. *Geol. Belgica* **2020**, *23*, 69–85. [[CrossRef](#)]
23. Batumike, M.J.; Kampunzu, A.B.; Cailteux, J.H. Lithostratigraphy, basin development, base metal deposits, and regional correlations of the Neoproterozoic Nguba and Kundelungu rock successions, Central African Copperbelt. *Gondwana Res.* **2007**, *11*, 432–447. [[CrossRef](#)]
24. François, A. *L'extrémité Occidentale de Larc Cuprifère Shabien. Etude Géologique. Mémoire du Département Géologique*; Éditeur Non identifié: Likasi, République du Zaïre, 1973; pp. 1–65.
25. Master, S.; Rainaud, C.; Armstrong, R.; Phillips, D.; Robb, L. Provenance ages of the Neoproterozoic Katanga Supergroup (Central African Copperbelt), with implications for basin evolution. *J. Afr. Earth Sci.* **2005**, *42*, 41–60. [[CrossRef](#)]

26. Mambwe, P.; Milan, L.; Batumike, J.; Lavoie, S.; Jébrak, M.; Kipata, L.; Chabu, M.; Mulongo, S.; Lubala, R.T.; Delvaux, D.; et al. Lithology, petrography, and Cu mineralization of the Neoproterozoic glacial Mwale Formation at the Shanika syncline (Tenke Fungurume, Congo Copperbelt; Democratic Republic of Congo). *J. Afr. Earth Sci.* **2017**, *129*, 898–909. [[CrossRef](#)]
27. Dewaele, S.; Muchez, P.; Vets, J.; Fernandez-Alonzo, M.; Tack, L. Multiphase origin of the Cu-Co deposits in the western portion of the Lufilian fold and thrust belt, Katanga (Democratic Republic of Congo). *J. Afr. Earth Sci.* **2006**, *46*, 455–469. [[CrossRef](#)]
28. Kampunzu, A.B.; Cailteux, J.L.H.; Kamona, A.F.; Intiomale, M.M.; Melcher, F. Sediment-hosted Zn-Pb-Cu deposits in the Central African Copperbelt. *Ore Geol. Rev.* **2009**, *35*, 263–297. [[CrossRef](#)]
29. François, A. Stratigraphie, tectonique et minéralisation dans larc cuprifère du Shaba3. In *Gisements Stratiformes et Provinces Cuprifères*; Bartholomé, P., Ed.; Centenaire de la Société Géologique de Belgique: Liège, Belgium, 1974; pp. 79–101.
30. Oosterbosch, R. Les minéralisations dans le système de Roan au Katanga. In *Gisements Stratiformes de Cuivre en Afrique*; Lombard, J., Nicolini, P., Eds.; 1ere Partie: Mons, Belgium, 1962; pp. 71–136.
31. Fontaine, L.; De Putter, T.; Bernard, A.; Decrée, S.; Cailteux, J.; Wouters, J.; Yans, J. Complex mineralogical-geochemical sequences and weathering events in the supergene ore of the Cu-Co Luiswishi deposit (Katanga, D.R. Congo). *J. Afr. Earth Sci.* **2020**, *161*, 103674. [[CrossRef](#)]
32. Charlet, J.M.; Quinif, Y.; Loris, N.B.T. The Luiswishi deposit, radiometry of the host rocks, relation to the U-Mineralizations. In *Gisements Stratiformes de Cuivre et Minéralisations Associées*; Charlet, J.-M., Ed.; Académie Royale des Sciences d’Outre-Mer: Colloque International Cornet: Mons, Belgium, 1997; p. 17.
33. Loris, N.B.T.; Charlet, J.-M.; Pechman, E.; Clare, C.; Chabu, M.; Quinif, Y. Caractéristiques minéralogiques, cristallographiques, physico-chimiques et âges des minéralisations uranifères de Luiswishi (Shaba, Zaïre). In *Gisements Stratiformes de Cuivre et Minéralisations Associées*; Charlet, J.-M., Ed.; Académie Royale des Sciences d’Outre-Mer: Mons, Belgium, 1994; pp. 285–306.
34. Welham, N.J.; Johnston, G.M.; Sutcliffe, M.L. AmmLeach (R): A New Paradigm in Copper–Cobalt Processing, Copper Cobalt Africa. In Proceedings of the 8th Southern African Base Metals Conference, Livingstone, Zambia, 6–8 July 2015.
35. Nisbett, A.; Baxter, K.; Marte, K.; Urbani, M. Flowsheet considerations for Cu Co projects. *J. S. Afr. Inst. Min. Metall.* **2009**, *109*, 641–646.
36. Ferron, C.J. The Control of Manganese in Acidic Leach Liquors, with Special Emphasis to Laterite Leach Liquors; SGS Minerals Services Technical Paper. 2002. Available online: <https://www.sgs.com/-/media/global/documents/technical-documents/sgs-technical-papers/sgs-min-tp2002-02-manganese-control-in-acidic-leach-liquors.pdf> (accessed on 23 February 2022).
37. Könighofer, T.; Archer, S.J.; Bradford, L. A Cobalt solvent extraction investigation in Africa’s Cu Belt. *J. S. Afr. Inst. Min. Metall.* **2009**, *109*, 337–342.
38. Swartz, B.; Donegan, S.; Amos, S. Processing considerations for Co recovery from Congolese Copperbelt ores, Processing considerations for Co recovery from Congolese Copperbelt ores. Hydrometallurgy Conference. *J. S. Afr. Inst. Min. Metall.* **2009**, *38*, 385–400.
39. Walraven, F.; Chabu, M. Pb-isotopic constraints on base-metal mineralization at Kipushi (Southeastern Zaire). *J. Afr. Earth Sci.* **1994**, *18*, 73–82. [[CrossRef](#)]
40. Hitzman, M.; Kirkham, R.; Broughton, D.; Thorson, J.; Selley, D. The sediment-hosted stratiform copper ore system. In *Economic Geology: One Hundredth Anniversary Volume, 1905–2005*; Hedenquidt, J.W., Thompson, J.F.H., Goldfarb, R.J., Richards, J.P., Eds.; Society of Economic Geologists: Littleton, CO, USA, 2005; pp. 609–642.
41. Sillitoe, R.H.; Perello, J.; Garcia, A. Sulfide-Bearing Veinlets Throughout the Stratiform Mineralization of the Central African Copperbelt: Temporal and Genetic Implications. *Econ. Geol.* **2010**, *105*, 1361–1368. [[CrossRef](#)]
42. Loris, N.B.T.; Charlet, J.M.; Okitaudji, R. La mobilité de l’uranium et des métaux associés en environnement géologique oxydo-réducteur, le cas des minéralisations Cu-Co-Ni-U de Luiswishi (Katanga, RDC). *Acad. Royal. Sci. Outre-Mer.* **2002**, *48*, 165–188.
43. El Desouky, H.A.; Muchez, P.; Boyce, A.J.; Schneider, J.; Cailteux, J.L.H.; Dewaele, S.; von Quadt, A. Genesis of sediment-hosted stratiform copper–cobalt mineralization at Luiswishi and Kamoto, Katanga Copperbelt (Democratic Republic of Congo). *Miner. Depos.* **2010**, *45*, 735–763. [[CrossRef](#)]
44. Mambwe, P.; Muchez, P.; Lavoie, S.; Kipata, L.; Dewaele, S. Evidence for late Lufilian orogenic mineralizing fluids at the Kamalondo Cu-Co deposit (Tenke Fungurume, Democratic Republic of the Congo). In Proceedings of the 15th SGA Biennial Meeting, Glasgow, UK, 27–30 August 2019; pp. 287–290.
45. Davey, J.; Roberts, S.; Wilkinson, J.J. Copper-and cobalt-rich, ultrapotassic bittern brines responsible for the formation of the Nkana-Mindola deposits, Zambian Copperbelt. *Geol. Soc. Am. Bull.* **2020**, *49*, 341–345. [[CrossRef](#)]
46. Schmandt, D.; Broughton, D.; Hitzman, M.W.; Plink-Bjorklund, P.; Edwards, D.; Humphrey, J. The Kamoa Copper Deposit, Democratic Republic of Congo: Stratigraphy, Diagenetic and Hydrothermal Alteration, and Mineralization. *Econ. Geol.* **2013**, *108*, 1301–1324. [[CrossRef](#)]
47. Hendrickson, M.D.; Hitzman, M.W.; Wood, D.; Humphrey, J.D.; Wendlandt, R.F. Geology of the Fishtie deposit, Central Province, Zambia: Iron oxide and copper mineralization in Nguba Group metasedimentary rocks. *Miner. Depos.* **2015**, *50*, 717–737. [[CrossRef](#)]
48. Mambwe, P.; Kipata, M.L.; Chabu, M.; Muchez, P.; Lubala, R.T.; Jébrak, M.; Delvaux, D. Sedimentology of the Shangoluwe breccias and timing of the Cu mineralization (Katanga Supergroup, D.R. of Congo). *J. Afr. Earth Sci.* **2017**, *132*, 1–15. [[CrossRef](#)]
49. Twite, F.; Broughton, D.; Nex, P.; Kinnaird, J.; Gilchrist, G.; Edwards, D. Lithostratigraphic and structural controls on sulphide mineralization at the KamoaCu deposit, Democratic Republic of Congo. *J. Afr. Earth Sci.* **2019**, *151*, 212–224. [[CrossRef](#)]

50. Twite, F.; Nex, P.M.A.; Kinnaird, J. Strain fringes and strain shadows at Kamoia (DRC), implications for copper mineralization. *Ore Geol. Rev.* **2020**, *122*, 103536. [[CrossRef](#)]
51. Chabu, M.; Boulègue, J. Barian feldspar and muscovite from the Kipushi Zn-Pb-Cu deposit, Shaba, Zaïre. *Can. Mineral.* **1992**, *30*, 1143–1152.
52. Chabu, M. The geochemistry of phlogopite and chlorite from the Kipushi Zn-Pb-Cu deposit, Shaba, Zaïre. *Can. Mineral.* **1995**, *33*, 547–558.
53. Haest, M.; Muchez, P.; Dewaele, S.; Boyce, A.J.; Von Quadt, A.; Schneider, J. Petrographic, fluid inclusion and isotopic study of the Dikulushi Cu-Ag deposit, Katanga (D.R.C.): Implications for exploration. *Miner. Depos.* **2009**, *44*, 505–522. [[CrossRef](#)]
54. Van Wilderode, J.; Heijlen, W.; De Muynck, D.; Schneider, J.; Vanhaecke, F.; Muchez, P. The Kipushi Cu-Zn deposit (DR Congo) and its host rocks: A petrographical, stable isotope (O, C) and radiogenic isotope (Sr, Nd) study. *J. Afr. Earth Sci.* **2013**, *79*, 143–156. [[CrossRef](#)]
55. Key, R.M.; Liyungu, A.K.; Njamu, F.M.; Somwe, V.; Banda, J.; Mosley, P.N.; Armstrong, R.A. The western arm of the Lufilian Arc in NW Zambia and its potential for copper mineralization. *J. Afr. Earth Sci.* **2001**, *33*, 503–528. [[CrossRef](#)]
56. Barron, J.W.; Broughton, D.W.; Armstrong, R.A.; Hitzman, M.W. Petrology, geochemistry and age of gabbroic bodies in the Solwezi area, northwestern Zambia. In Proceedings of the 3rd IGCP-450 Conference, Proterozoic Sediment-Hosted Base Metal Deposits of Western Gondwana, Conference and Field Workshop Lubumbashi 2003, Lubumbashi, Democratic Republic of Congo, 14–24 July 2003; pp. 75–77.
57. Rooney, A.D.; Strauss, J.V.; Brandon, A.D.; McDonald, F.A. A Cryogenian chronology: Two long-lasting synchronous Neoproterozoic glaciations. *Geol. Soc. Am. Bull.* **2015**, *43*, 459–462. [[CrossRef](#)]
58. Mambwe, P. Sédimentologie et Minéralisation Cuprifère Associée au Groupe du Kundelungu. Cas du Gisement de Shangoluwe (Kambove, RDC). Inclusions Fluides et Contrôle Tectonique. Master's Thesis, University of Lubumbashi, Lubumbashi, Democratic Republic of Congo, 2017. Unpublished Work.
59. Shengo, M.L.; Kitobo, S.W.; Kime, M.B.; Mambwe, M.P.; Nyembo, T.K. Mineralogical variations with the mining depth in the Congo Copperbelt: Technical and environmental challenges in the hydrometallurgical processing of Cu and Co ores. *J. Sustain. Min.* **2020**, *19*, 96–114.
60. Zientek, M.L.; Bliss, J.D.; Broughton, D.W.; Christie, M.; Denning, P.D.; Hayes, T.S.; Hitzman, M.W.; Horton, J.D.; Frost-Killian, S.; Jack, D.J.; et al. *Sediment-Hosted Stratabound Copper Assessment of the Neoproterozoic Roan Group, Central African Copperbelt, Katanga Basin, Democratic Republic of the Congo and Zambia*. Global Mineral Resource Assessment; Science Investigation Report 2010-590-T; U.S. Geological Survey: Reston, VI, USA, 2014; p. 162.
61. Jinchuan Group International Resources Co. Ltd. *A Competent Person's Report and Valuation Report on the Mineral Assets of METOREX (PTY) Ltd in the Democratic Republic of Congo and the Republic of Zambia*; Report Prepared by SRK Consulting: Denver, CO, USA, 2013; p. 810.
62. Taylor, C.D.; Causey, J.D.; Denning, P.D.; Hammarstrom, J.M.; Hayes, T.S.; Horton, J.D.; Kirschbaum, M.J.; Parks, H.L.; Wilson, A.B.; Wintzer, N.E.; et al. *Descriptive Models, Grade-Tonnage Relations, and Databases for the Assessment of Sediment-Hosted Copper Deposits—With Emphasis on Deposits in the Central Africa Copperbelt, Democratic Republic of the Congo, and Zambia*; U.S. Geological Survey Scientific Investigations Report 2010-5090-J; U.S. Geological Survey: Reston, VA, USA, 2013; p. 154.
63. Haest, M.; Muchez, P. Stratiform and vein-type deposits in the Pan-African Orogen in Central and Southern Africa: Evidence for multiphase mineralization. *Geol. Belg.* **2011**, *14*, 23–44.
64. Lefebvre, J.J.; Cailteux, L.H. Volcanisme et mineralizations diagenétiques dans le gisement de l'Etoile, Shaba, Zaïre. *Ann. Soc. Géol. Belg.* **1975**, *98*, 177–195.
65. Berkman, D.A. *Field Geologist's Manual*, 4th ed.; Australian Institute of Mining and Metallurgy: Carlton, Australia, 2001; p. 395.
66. Long, G.; Peng, Y.P.; Dee Bradshaw, D. A review of copper–arsenic mineral removal from copper concentrates. *Miner. Eng.* **2012**, *36–38*, 179–186. [[CrossRef](#)]
67. Van Langendonck, S.; Muchez, P.; Dewaele, S.; Kaputo, A.K.; Cailteux, J. Petrographic and mineralogical study of the sediment-hosted Cu-Co ore deposit at Kambove West in the central part of the Katanga Copperbelt (DRC). *Geol. Belg.* **2013**, *16*, 91–104.
68. Mbuya, B.I.; Kime, M.B.; Ntakamutshi, P.T.; Mwilen, T.R.; Muhungu, S.T.; Mwema, E.M.; Kanda, J.M.N.; Kaniki, A.T. Evaluation of flocculation and settling behavior of leach residues: Contribution of principal component analysis. *J. Sustain. Metall.* **2018**, *4*, 485–492. [[CrossRef](#)]
69. Parviainen, A.; Soto, F.; Caraballo, M.A. Revalorization of Haveri Au-Cu mine tailings (SW Finland) for potential reprocessing. *J. Geochem. Explor.* **2020**, *218*, 106614. [[CrossRef](#)]
70. Velásquez, G.; Estay, H.; Vela, I.; Salvi, S.; Pablo, M. Metal-selective processing from the Los Sulfatos Porphyry-Type Deposit in Chile: Co, Au, and Re recovery workflows based on advanced geochemical characterization. *Minerals* **2020**, *10*, 531. [[CrossRef](#)]
71. Brest, K.K.; Henock, M.M.; Guellord, N.; Kimpiab, M.; Kapiamba, K.F. Statistical investigation of flotation parameters for copper recovery from sulfide flotation tailings. *Results Eng.* **2021**, *9*, 100207. [[CrossRef](#)]
72. Shengo, L.M. Potentially exploitable reprocessing routes for recovering copper and cobalt Retained in Flotation Tailings. *J. Sustain. Metall.* **2021**, *7*, 60–77. [[CrossRef](#)]
73. De Putter, T.; Ruffet, G.; Yans, J.; Mees, F. The age of supergene manganese deposits in Katanga and its implications for the Neogene evolution of the African Great Lakes Region. *Ore Geol. Rev.* **2015**, *71*, 350–362. [[CrossRef](#)]

74. Decrée, S.; Pourret, O.; Baele, J.M. Rare earth element fractionation in heterogenite (CoOOH): Implication for cobalt oxidized ore in the Katanga Copperbelt (Democratic Republic of Congo). *J. Geochem. Explor.* **2015**, *159*, 290–301. [[CrossRef](#)]
75. Decrée, S.; Deloule, E.; De Putter, T.; Dewaele, S.; Mees, F.; Baele, J.M.; Marignac, C. Dating of U-rich heterogenite from the Katanga Copperbelt: New insights into U deposit genesis and U cycling. *Precambrian Res.* **2014**, *241*, 17–28. [[CrossRef](#)]
76. Cailteux, J. L'origine du talc dans le C.M.N. (ou R.2.3) de Kambove (Shaba-Zaire). *Ann. Soc. Géol. Belg.* **1979**, *102*, 213–221.
77. Mbuya, B.I.; Kime, M.B.; Kabeya, C.M.; Kaniki, A.T. Clarification and solvent extraction studies of a high talc containing copper aqueous solution. *J. Mater. Res. Technol.* **2018**, *7*, 218–222. [[CrossRef](#)]
78. Shengo, M.L.; Kime, M.B.; Mambwe, M.P.; Nyembo, T.K. A review of the beneficiation of Cu-Co-bearing minerals in the Democratic Republic of Congo. *J. Sustain. Min.* **2019**, *18*, 226–246. [[CrossRef](#)]
79. Sośnicka, M.; Gigler, G.M.; Kinnaird, J.A.; Przybyłowicz, W.J.; Chimving, J.; Master, S.; Plessen, B. Mineralizing fluids of the supergene-enriched Mashitu South Cu-Co deposit, Katanga Copperbelt, DRC. *Ore Geol. Rev.* **2019**, *109*, 201–228. [[CrossRef](#)]
80. Gigler, G.M.; Kinnaird, J. Element mobility in the weathering environment and surface vectors to mineralization—A case study from the Mashitu South Cu-Co deposit, Katanga, Democratic Republic of Congo. *J. Geochem. Explor.* **2017**, *183*, 127–137. [[CrossRef](#)]
81. Loris, N.B.T.; Charlet, J.-M.; Kanzundu, M.; Cailteux, J.L.H.; Kampunzu, A.B. Distribution of uranium in the Luishia Cu-Co stratiform deposits (Katanga, RDC) and genetic implications. In Proceedings of the Abstracts of the IGCP 450 Conference and Field Workshop, Lubumbashi, Democratic Republic of Congo, 14–24 July 2003; pp. 108–112.
82. Ngongo, K. Similarity Between the uraniferous deposits (Shinkolobwe type) and the cupriferous deposits (Kamoto type) at Shaba, Zaire. *Ann. Soc. Géol. Belg.* **1975**, *98*, 449–462.
83. Decrée, S.; Deloule, É.; De Putter, T.; Dewaele, S.; Mees, F.; Yans, J.; Marignac, C. SIMS U–Pb dating of uranium mineralization in the Katanga Copperbelt: Constraints for the geodynamic context. *Ore Geol. Rev.* **2011**, *40*, 81–89. [[CrossRef](#)]
84. Debruyne, D.; Balcaen, L.; Vanhaecke, F.; Muchez, P. Rare earth element and yttrium characteristics of carbonates within the sediment-hosted Luiswishi and Kamoto Cu-Co deposits, Katanga Copperbelt (Democratic Republic of Congo—DRC). *Geol. Belg.* **2013**, *16*, 76–83.
85. Moskalyk, R.R.; Alfantazi, A.M. Review of present cobalt recovery practice. *Miner. Metall. Process.* **2000**, *17*, 205–216.
86. Jurrius, Y.; Sole, K.C.; Hardwick, E. Removal of Cu and zinc from a Co electrolyte by ion exchange at Kamoto Cu company's Luilu plant. In Proceedings of the 7th International Symposium, Hydrometallurgy 2014—Volume II, Victoria, BC, Canada, 22–25 June 2014; Canadian Institute of Mining, Metallurgy and Petroleum: Montreal, QC, Canada, 2014; pp. 281–293.
87. Vanbrabant, Y.; Burlet, C.; Louis, P. Mineralogical Characterization of Cobaltic Oxides from the Democratic Republic of Congo. In *Ni-Co 2013*; John Wiley and Sons Inc.: Hoboken, NJ, USA, 2013; pp. 241–254.
88. Macfarlane, A.S.; Willians, T.P. Optimizing value on a copper mine by adopting a geometallurgical solution. *J. S. Afr. Inst. Min. Metall.* **2014**, *114*, 929–936.